Accepted Manuscript

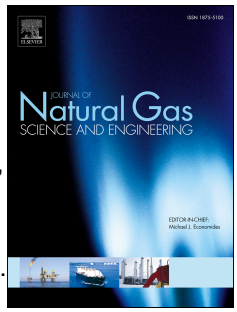

Lithological and facies analysis of the Roseneath and Murteree shales, Cooper Basin, Australia

Quaid Khan Jadoon, Eric Roberts, Bob Henderson, Thomas Blenkinsop, Raphael A.J. Wüst, Cassy Mtelela

PII: S1875-5100(16)30785-5

DOI: 10.1016/j.jngse.2016.10.047

Reference: JNGSE 1893

To appear in: *Journal of Natural Gas Science and Engineering*

Received Date: 3 March 2016

Revised Date: 20 October 2016

Accepted Date: 24 October 2016

Please cite this article as: Jadoon, Q.K., Roberts, E., Henderson, B., Blenkinsop, T., Wüst, R.A.J., Mtelela, C., Lithological and facies analysis of the Roseneath and Murteree shales, Cooper Basin, Australia, *Journal of Natural Gas Science & Engineering* (2016), doi: 10.1016/j.jngse.2016.10.047.

Lithological and facies analysis of the Roseneath and Murteree shales, Cooper Basin, Australia

Quaid Khan Jadoon[1]*, Eric Roberts [1], Bob Henderson[1],Thomas Blenkinsop[1,2], Raphael A. J. Wüst[1, 3], Cassy Mtelela[1]

[1]*Department of Geosciences College* of Science, Technology & Engineering *James Cook University, Douglas Townsville, Queensland 4811, Australia*

[2]*School of Earth and Ocean Science Cardiff University Main building, Park Place Cardiff CF10 3AT United Kingdom*

[3]*Trican Geological Solutions, 621-37th Avenue NE Calgary, Alberta, Canada T2E2M1*

Corresponding Author: quaid.jadoon@my.jcu.edu.au

ABSTRACT

Unconventional shale plays have received marked attention over the last five years because of their economic potential for hydrocarbon generation, and yet they are amongst the least understood of all clastic sedimentary rock systems. The Cooper Basin is one of the largest Gondwana intracratonic basins in Australia, extending from northern South Australia into south-western Queensland and covering approximately 130,000 km^2. The basin is may be prospective for shale gas, particularly within the lacustrine shales of the Permian Murteree and Roseneath formations. This study investigates lithological characteristics of these two units in relation to reservoir evaluation. Core samples representing the Dirkala-02 and Moomba-46 wells were used for petrographic analysis. A combination of wireline log analysis, thin section petrography, X-ray diffraction and pyrolysis analysis was used to define and characterize four distinct lithofacies facies within the Roseneath and Murteree shales: siliceous mudstone, organic siliceous mudstone, calcareous siliceous mudstone, and silty siliceous mudstone. The siliceous mudstone and organic siliceous mudstone are the most common. Diagenetic siderite occurs in all four lithofacies. A conceptual depositional model is developed for deposition of the Roseneath and Murteree shales. Wireline-log cross plots were interpreted and utilized in the construction of electrofacies. The study was concentrated on the northern portion of the basin between the Nappameri and Patchawarra Troughs in order to understand the nature of lithofacies and variability in reservoir architecture, which was controlled by relative lake level fluctuation. The results of this study will aid in the evaluation of shale gas potential for this portion of the basin, as well as a better understanding of shale gas opportunities in the Cooper Basin more generally.

Keywords: Shale Gas, Lithofacies, Electrofacies, Roseneath, Murteree, Permian, Cooper-Basin.

1. Introduction

Advancements in drilling and well completion techniques over the last 20 years have resulted in the exploration of many unconventional liquid and gas reservoirs around the globe (Wust et al., 2015). Unconventional hydrocarbon reservoirs differ from conventional reservoirs in that they commonly represent both source and reservoir for hydrocarbon generation and accumulation. During burial and diagenesis, some hydrocarbons may be lost due to migration, but much remains in place due to the low permeability of the host rock (Myers, 2008). To date, unconventional shale gas has mostly been developed in North America, with a minimal exploitation of this resource in other parts of the world.

The Cooper Basin (Fig. 1) is the largest onshore petroleum province in Australia and has both conventional and unconventional reservoirs (Hill and Gravestock, 1995). Its sedimentary succession hosts a significant amount of Australia's onshore oil and gas, which has been in production since 1963, mainly for natural gas (with some liquids). The main hydrocarbon reservoir intervals in the basin are located within the Late Paleozoic Gidgealpa Group (Fig. 2). The Cooper Basin is widely regarded as one of the most prospective basins in Australia for shale gas. Unlike most other unconventional shale gas plays in North America and elsewhere, the Cooper Basin consists entirely of non-marine strata. Its hydrocarbons are derived from a range of terrestrial organic sources, including coal beds. Liquid hydrocarbons from the Patchawarra and Toolachee formations are isotopically lighter in character than liquid hydrocarbons from other units in the basin (Boreham and Summins, 1999). This difference has been interpreted to be the result of differing organic sources, suggesting two independent petroleum systems within the basin. Basin analysis and evaluation of hydrocarbon potential for the Cooper Basin is especially challenging because it is entirely covered at present with no surface expression. This makes certain exploration techniques, especially analysis of core and wireline logs, particularly critical since outcrop exposures are unavailable for study. Where core samples are not available, electrofacies derived from down-hole wireline logs, based on input parameters of wells with both core and log data, are extremely helpful in the evaluation of lithological models basin-wide.

Well log cluster analysis is used to evaluate similarities/dissimilarities between data points in the multivariate space of logs, in order to group them into electrofacies (Euzen et al, 2010). The prediction is made by computing the probability of each data point for a certain defined electrofacies (Fourier, 1997). The most important outcome of electrofacies analysis is the determination of the probable lithofacies types that correspond to each electrofacies, based on analysis of known lithofacies

characteristics in key test wells and conducting clustering and discrimination analysis of test wells vs. unknown wells (i.e. uncored or undescribed). Electrofacies modelling is used to develop a conceptual geological model of the lithofacies in areas without cored wells with the help of conventional well log data and assigned lithofacies in these wells (e.g. Faliven et al., 2006; Deutsch, 2002; Qiet et al., 2007; Schlumberger, 2011; Galli et al., 1994; Eschard et al., 1998). To achieve this, stochastic and deterministic modelling approaches are used to subdivide electrofacies into pixel-based and object-based lithofacies. (Bret et al., 1996) (Lash et al., 2011). Dong et al. (2013) proposed an improved method for doing this based on K-means, which uses the optimized initial K-mean algorithm (one of the most popular and widespread partitioning clustering algorithms) to identify and cluster groups together in to classes and establish a set of input points for electrofacies (Khedairia and Khadir, 2008).

On the basis of detailed petrographic analysis of samples from two wells cored through the Permian Murteree and Roseneath shales (Dirkala-02 and Moomba-46 wells), four lithofacies have been recognized. Core descriptions were performed focusing on texture, lithology, bioturbation and sedimentary structure. The lithofacies were classified on the basis of quartz-mud ratio, grain size, sedimentary structures and organic matter. In each well, the recovered cores covered only short sections of the Roseneath and the Murteree formations. Petrographic and geochemical analyses of core samples were used to develop the electrofacies and these were used to extend the facies interpretations for Roseneath and Murteree shales across the basin into areas where the core was not available for study. Hence, the electrofacies mapping and correlation were also used to recognize reservoir attributes within the Roseneath and Murteree shales, which provide a way of targeting hydrocarbons in these portions of the basin. Although the sedimentology of these Permian shales have been investigated by more traditional means in the past, the combined lithofacies/electrofacies approach applied in this study represents an important advance in understanding and correlating strata across the basin and for improving our understanding of favorable target intervals in the unconventional shale gas target sequences of the Roseneath and Murteree formations in the Cooper Basin.

2. Geological setting of the Cooper Basin

The Cooper Basin is an intracratonic rift basin of Permo-Triassic age that extends from the northeastern corner of South Australia into southwestern Queensland (Klemme, 1980) (Fig. 1). The basin covers an area of approx. 130,000 sq. km; ~35,000 sq. km of which are in northeastern South Australia. Three major troughs, the Patchawarra, Nappamerri, and Tenappera Troughs, separated by structural ridges of Gidgealpa, Merrimelia, Innaminka and Murteree, are the major structural features of the basin. Each of these troughs has a Permo-Carboniferous to Triassic section up to 2500 m thick, and is overlain by up to 1300 m of Jurassic to Tertiary cover. The Murteree ridge post-dates infill of the basin and is associated with the reactivation of NW-trending thrust faults in the underlying Warburton Basin (Wopfner, 1972) (Fig. 2).

The basin fill is composed of a large number of non-marine depositional units of the Late Permian Gidgealpa Group and the Late Permian to Middle Triassic Nappamerri Group (PIRSA, 2000). The Neoproterozoic–Ordovician Warburton Basin and younger granitoids underlie the Cooper Basin sequence (Klemme, 1980, Radkeet et al., 2012). The unconformity separating the Cooper Basin from older rocks is interpreted to have resulted from the Devonian-Carboniferous Alice Springs Orogeny. Overlying and extending beyond the Cooper Basin are Jurassic-Cretaceous cover sequences of the Eromanga Basin, which form part of the Great Artesian Basin of eastern Australia.

The basal unit in the Cooper Basin is the Merrimelia Formation, which is considered the economic basement for hydrocarbon exploration (Williams and Wild, 1984; Williams et al., 1985) (Fig. 2). This unit is late Carboniferous to Early Permian in age based on palynology (Price et al., 1985) and consists of conglomerate, sandstone and shale deposited in glacial environments. A variety of depositional settings is inferred, including glacial valleys, braid plains, and lakes, which are together characterized by complex facies relationships and irregular thicknesses (Williams et al., 1985).

The succeeding Tirrawarra Sandstone is characterized by thick, multi-story channel sandstones with distinctive quartz arenite compositions (Kapel, 1972; Gostin, 1973; Thorton, 1979). The Patchawarra Formation, which overlies this, is the thickest unit in the Cooper Basin, although it shows great lateral thickness variation (Gatehouse, 1972). It is thickest in the Nappamerri and Patchawarra Troughs and thins by onlap and truncation onto the crests of major structures and at the basin margins (Batterby, 1976). It represents a succession of massive cross-bedded fluvial sandstones with minor channel lag conglomerates. The Patchawarra Formation has also laminated siltstones, shales and coals that formed in abandoned channels, shallow lakes and peat swamps. The overlying Murteree, Epsilon, Roseneath and Daralingie Formations record alternating lacustrine and lower delta plain deposition and

consist mainly of interbedded fluvial-deltaic sandstones, shales, siltstones and coals (Kapel, 1972; Gostin, 1973; Thorton, 1979).

The Murteree Shale was defined by Gatehouse (1972) as a shale interval overlain by the Epsilon Formation and underlain by the Patchawarra Formation. This unit consists of black to dark grey to brown argillaceous siltstone and fine-grained sandstone, which becomes sandier in the southern Cooper Basin. Fine-grained pyrite and muscovite are both characteristic of the Murteree Shale and significant carbonaceous siltstone is also present. The type section lies between 1922.9 and 1970.8 m in the Murteree 1 well. The unit is widespread within the Cooper Basin in both South Australia and Queensland. It is relatively uniform in thickness, averaging ~50 m and reaching a maximum thickness of 86 m in the Nappameri Trough. It thins to the north and is only 35 m thick in the Patchawarra Trough and absent over the crestal ridges (Boucher, 2000). The Murteree Shale is early Permian (Price et al., 1985), and is interpreted as a relatively deep lacustrine depositional environment, in part based on the rarity of wave ripples and lack of other evidence of storm reworking (Gravestock et al., 1995).

The Roseneath Shale was defined by Gatehouse (1972) as a suite of shales and minor siltstones that conformably overlie, and intertongue with, the Epsilon Formation. The unit was originally included as one of three units in the Moomba Formation by Kapel (1972); however, Gatehouse (1972) raised it to formation status. The type section lies between 1956.8 – 2024.5 m in the Roseneath 1 well (Gatehouse, 1972). The Roseneath Shale is composed of light to dark brown-grey or olive-grey siltstones and mudstones with minor fine-grained pyrite and pale brown sandstone interbeds. It occurs across the central Cooper Basin but has been eroded from the Dunoon and Murteree Ridges and crestal areas of other ridges during late Early Permian uplift. The Roseneath Shale reaches a thickness of 105 m in the Strathmount-1 well and is thickest in the Nappamerri and Tenappera Troughs (Boucher, 2000). The Roseneath Shale is not as extensive as the Murteree Shale. It is overlain by and also intertongues with the Daralingie Formation. Where the latter has been removed by erosion, the Roseneath Shale is unconformably overlain by the Toolachee Formation. The unit is considered to be Early Permian in age (Kungurian; pp3 to pp4 palynozones of Price et al., 1985), and is interpreted as a lacustrine depositional environment, similar to that of the Murteree Shale (Stuart, 1976; Thorton, 1979). Variations between massive to finely laminated intervals, with minor wavy lamination and wave ripples, suggest lake bottom sediment reworking. These features, as well as load, flame and slump structures, suggest a shallower water lacustrine setting than that of the Murteree Shale (Stuart, 1976; Thorton, 1979).

3. Background of depositional environments and paleoclimate

Depositional history in the Cooper basin started during the late Carboniferous. During the late Carboniferous, the Antarctic ice sheet reached a maximum volume before it retreated during the early Permian (Veevers and Powell, 1987). Ice brought tremendous volumes of marine and non-marine sediments into the Gondwana basin (Gilby et al., 1988). During the Permian, the basin structure and the water masses controlled the mixed lake-fluvial deposits of the REM (Roseneath, Epsilon, and Murteree).

The paleo-environmental evolution of the Cooper Basin around the time of deposition of the Roseneath and Murteree shales is schematically illustrated in four block diagrams (Fig. 3): a) During late Carboniferous time, the Gondwana continental ice sheet covered most of the basin (Merrimelia ice sheets) (Crowell and Frakes, 1971). The Merrimelia Formation deposition coincided with the Gondwana glacier maximum when Australia and the Cooper Basin were situated in high southern polar latitudes (Veevers and Powell, 1987); b) During the Late Carboniferous, the Merrimelia ice sheet waned and retreated. Abundant coarse grained fluvial deposits were shed into the basin where rapid lateral and vertical accretions due to variation in melt water volume occurred (Chaney, 1998). Continuous fluvial influx led to deposition of thick Tirrawara sandstones (Alley, 1995); c) Transition to lacustrine and cold climate fluvial deposition with peat swamps in marginal zones (Patchawarra Formation); d) Lake development and deposition of Roseneath and Murteree shales in a broad fresh water lake (Stuart,1976).The Late Permian was characterised by anoxic to aerobic bottom conditions. Sedimentation in the lake depended on the suspension and flux of sediments. The evidence and deposition of the Roseneath and Murteree shales presented by other workers in many analogous setting. (William, 1995; Gravestock and Morton, 1983; Staurt, 1976; Thorton, 1979) for both the Murteree and Roseneath shales.

The Murteree Shale was deposited in a broad, fresh water lake (Staurt, 1976) that was deeper than the lake from which the Roseneath Shale was deposited. Wave ripples, soft sediment deformation, low angle cross bedding, planar lamination and occasional turbidites and rhythmites (William, 1995) are all observed together with slump folds and micro faults that indicate slope instability conditions (Grave et al., 1984). Burrowing and dropstones are also observed in large quantity. These are related ice or vegetation rafting (Alexander, 1988) lack of biota, but evidence of full of bioturbation in the Murteree and Roseneath shales. According to Williams (1995), the shoreface lake delta slope and prodelta environment in the cores samples that are attributes of the gravity flow or distal turbidites affected by seasonal influence.

The Roseneath Shale varies from massive to finely laminate with occasional load marks, slump folds, and flame structures also indicating common mass flows and slope instability conditions during deposition (Stuart, 1976). The Roseneath depositional environment was similar to the one during deposition of the Murteree Shale (Stuart, 1976; Thornton, 1979). Both shales facies contain sedimentary structures created by turbidity currents and other gravity flows as well as pelagic sediments or suspension sedimentation, settling debris or gravity flow. The mudstone formed mainly from suspension settling. These suspended sediments were derived from pelagic and hemipelagic mud plumes from the lake shoreline (Fig. 4).

The sediments are generally coarsening upward with a moderate sand to shale ratio. Sedimentary structures in the Epsilon Formation consist of climbing ripples (tidal bundle), convolute bedding and some wavy lamination, mudstone with bioturbation and soft sediment deformation that disrupts bedding. (Fairburn, 1992) (Taylor et al., 1991). The occasional occurrence of low angle climbing ripple marks shows rapid deposition from decelerating flows, which are associated with river flood events (Ashley et al., 1982). The alternating sandstone and mudstone in the Epsilon Formation indicates fluctuating energy regimes. The fluctuation of energy played a vital role in the deposition; the low bioturbation suggests stressed conditions caused by the variation.

The regional transgressions and regressions during the deposition of Roseneath- Epsilon and Murteree Formations suggest an open basin setting (Thorton and Staurt 1976). When the Epsilon Formation was being deposited, a delta prograded westward of the lake and retreated to the east. Fairburn (1992) described the three depositional stages of Epsilon Formation, a lower lake shoreline facies, a middle deltaic unit, and an upper lake shoreline unit. The lower and upper stages were associated with regression during the time of the Murteree and Roseneath shales while during deposition of the Epsilon Formation, a fluviodeltaic facies prograded in the lake environment (Stuart, 1976; Fairburn, 1992). Clastic sedimentation involved more humid periods, where sands were eroded and transferred to the adjacent lacustrine basin by low gradient fluvial systems.

Recent research in eastern Australian has established that rather than being a single, long-lived epoch, the late Paleozoic ice age comprised of a series of glacial intervals each 1-8 Ma in duration, separated by non-glacial intervals of comparable duration. Eight discrete glacial events were recognized by Fielding et al. (2008a) from the stratigraphic record in New South Wales and Queensland. According to Fielding (2008b) glaciers gradually expanded in volume and geographical extent in eastern Australia through the Pennsylvanian to the Early Permian, reaching the highest stage of development in the late

Permian and waning through the Middle Permian. These patterns indicate that the late Paleozoic Ice Age was considerably more active than previous.

4. Methods and Data

This study presents an integrated analysis of core samples (geochemistry, mineralogy) and wireline logs for the development of lithofacies and electrofacies to model reservoir architecture structures (Fig. 5). Wireline log data, including gamma ray (GR), sonic (DT), and density (Rhob), neutron logs (NPHI) and drill core samples from two wells in the Nappameri trough (Dirkala-2 well) and Patchwarra trough (Moomba-46 well) are used (see Figs. 5-7a-b for details of sampling). The Moomba-46 well was drilled as a development well 9 km south of the Moomba gas plant on the South Dome of the Moomba Field. Dirkala-2 well was drilled in Murta block, located in a saddle, on the Dirkala anticline dome, 1.3 km NW of Dirkala. The Dirkala Field is located on a northeast-southwest trending structural high known as the Wancoocha Nose. Gamma-ray and sonic logs of the Roseneath and Murteree shales (Figs. 6 and 8) provide the basis for correlation of these units across the Cooper Basin. Core plugs were sampled at the Department of Manufacturing, Innovation, Trade, Resources and Energy (DIMITRE) South Australia, and Queensland Department of Natural Resources and Mines (DNRM) core library facilities.

Lithological data were collected from 54 core samples, made into thin sections. The goal of the optical microscopy was to understand and characterize the petrophysical properties of the two shales, including mineralogical composition, texture, porosity, diagenetic processes, and organic maturity to better understand the reservoir characteristics of the study units. TOC (total organic carbon) and Tmax data were measured on a Source Rock Analyzer at Trican Alberta Calgary laboratory and used to model log derived TOC for portions of the Roseneath and Murteree Shales where no samples were available. The TOC is used to help interpret the preliminary hydrocarbon generation potential across the basin. X-ray diffraction (XRD) analysis was performed on 34 replicate samples at Trican to better define the shale mineralogy. Sample material was micronized and smeared to prepare slides for analysis. Spectra were collected between 3 and 70^0 2Θ using a Bruker® D4 Endeavour instrument with a Lynx-Eye detector. The instrument was run at 40 kV and 30 mA and features a fixed divergence slit geometry (0.50), an anti-scatter slit with both primary and secondary Soller slits at 4^0 Θ. XRD data were analyzed using PDF-4 minerals database 2013 (peak identification) and quantified using Jade 9 software.

The core data were correlated with wireline data from Moomba-46 and Dirkala-2 wells and used to identify the characteristic log responses in order to correlate core and well log data across the basin. Core attributes were determined by matching the response of specific logs with the

lithology observed from the core. The lithofacies were correlated with wireline log data GR, RHOB, and DT logs and used to model electrofacies for the Roseneath and Murteree shales. Wireline data (Log ASCII Standard-LAS files) for GR, RHOB and DT were loaded into Senergy's software suite, Interactive Petrophysics (IP) 4.3. Data were first edited and reviewed, and then integrated for electrofacies recognition of the Roseneath and Murteree shales in the Moomba-46 and Dirkala-2 wells. The electrofacies identified in this analysis were then matched to lithological data. To facilitate the matching process, a cluster analysis was employed. The cluster analysis module of IP 4.3 version was used to cluster the data into groups to produce multivariate database zones and multi-curve cross plots, which can be used to correlate to geological facies. Basic steps involved in cluster analysis are as follows. Firstly, a database of attribute measurements was compiled for the objects to be calculated. Then a matrix of similarities or statistical distances between the objects was computed on the basis of the collective treatment of the attributes. The log curves were then normalized on standard deviation and principal component analysis was performed using the K-Mean clustering method. The resultant clusters were then observed through dendrograms and final clusters were calculated. The identified clusters were finally assigned a facies type.

Two neural network analysis methods were performed to interpret facies association in the uncored well sections of the Roseneath and Murteree shales across the study area. The first neural network analysis was an unsupervised method, where the sections were divided into several classifications based on the values of sonic, gamma ray and density logs. The second neural network analysis was supervised, where the classifications were defined by the result of facies associations interpreted from the core sections. These analyses identified the general log patterns, which were used to define and correlate specific facies (linked to their interpreted depositional environments) across the basin into areas where only wireline logs were available. Finally, the classification results acquired by clustering were each assigned a different colour scheme. These clusters are then either manually or automatically regrouped into the geological cluster. These electrofacies were coded in different colours as A: dark brown, B: yellow, C: red, and blue. Figure 8 summarizes the approaches used in this study involving the integration of core data lithofacies, conventional wireline logs data and electrofacies modeling.

5. Facies analysis of Roseneath and Murteree shales

The Murteree and Roseneath samples are all fine-grained mudstones with little textural variability. They are subtly to moderately laminated, organic-rich shales and siliceous mudstones. Based on petrographic investigations four lithofacies were identified as followings: 1) siliceous mudstone (SM), 2) organic siliceous mudstone (OSM), 3) silty siliceous mudstone (SSM), and 4) calcareous siliceous mudstone (CSM). All four lithofacies occur in both the Roseneath and Murteree shales (Figs. 9-12).

5.1 Siliceous mudstone (SM)

Description:

The siliceous mudstone facies (SM) is composed of horizontally laminated organic-rich siltstones, with weak bedding and is characterized by dark grey to black laminated quartz-rich intervals (Figs. 9c and 9g). Silt-sized quartz grains represent over half the composition (55%), with the remainder being clay. Quartz grains are sub-angular to sub-rounded, constituting both monocrystalline and polycrystalline varieties. Feldspars and rock fragments are essentially absent. Muscovite laths are common accessories and silt-sized authigenic montmorillonite grains are rare (Figs.9e, f). The clay minerals are dominated by illite and kaolinite minerals, which cover all grain contacts. Siderite in mostly microcrystalline habits is also observed (Figs.9h, i). Organic matter (OM) is weakly disseminated throughout this facies, but the total organic carbon (TOC) in is low (1.0 to 4.5 wt-% (Tables 1-2). Other distinctive features associated with the SM are quartz filled microfractures, which are common in this facies compared to the other facies. Bioturbation is very common in all core samples that were observed. In both formations, the proportion of SM increases towards the top of each unit. SM represents about ~20-25% of all lithofacies present in the Murteree, but only ~10-15% of lithofacies present in the Roseneath.

Interpretation:

The high quartz content is the most distinctive feature of the siliceous mudstone facies (SM), representing the most nearshore depositional environment in the study area. It is interpreted to have been deposited by suspension settling in a lacustrine depositional setting where abundant detrital silt-sized quartz particles, clay, and organic matter were present. The finely laminated nature of the facies and the presence of bioturbation is interpreted to represent deposition in a low-energy profundal setting. However, the alternation between silt- and clay-dominated laminations indicates alternating energy regimes during the deposition, which may be a result of periodic storm activity, and hence indicative of a moderately shallow setting not too far from paleo-shorelines.

5.2 Organic siliceous mudstone (OSM)

Description:

The organic siliceous mudstone facies (OSM) is characterized by dark grey to black, massive, organic-rich mudstone. It is slightly coarser grained in the Roseneath Shale than in the Murteree Shale, with common silt-size angular to rounded quartz and feldspar grains, which are patchy in distribution (Figs. 10a - i). Clay minerals include illite and kaolinite as well as muscovite and other indeterminate mica lathes. Quartz forms up to 40% of the samples, with similar amounts of clay minerals plus micas (Table 1). Siderite cement is present in all units and siderite concretions comprise nearly 10 to 15% of the Murteree Shale. Highly disseminated organic matter is relatively abundant (2.0 to 4.5%) in this facies; more than in any of the other lithofacies (Tables 1–2). In the Murteree Formation, the organic matter ranges from ~2% at a depth of 1894.7m, and reaches a maximum of 4.5% between 1897.7 and 1897.15m depths (Table 2). The Murteree Shale has the amorphous organic matter that is typically dark grey to black and preserved in horizontally laminated bands oriented parallel to bedding. The visible porosity is less than 2% and pore types include intercrystalline micropores. In general, the Murteree Shale yields a higher proportion of OSM than the Roseneath Shale. In both shales, the proportion of OSM increases towards the top of each formation. OSM represents about 4 to 5% of the lithofacies present in the Murteree, whereas it only represents 3 to 4% of lithofacies present in the Roseneath.

Interpretation:

The high organic content is the most diagnostic feature of the organic siliceous mudstone lithofacies that represents a deep water facie. The small particle sizes, the laminated nature combined with finely dispersed organics indicate a lower energy depositional setting and hence a more distal, deeper water pofundal environment is inferred. Rapid influxes of terrigenous sediment may be associated with some form of density current or distal turbidity currents. The high organic content indicates generally dysoxic to anoxic lake bottom conditions; however, the presence of bioturbation in some of the samples indicates that the lake bottom was not completely anoxic at this time. The origin of the organic matter is difficult to determine from thin section studies, because of the opaqueness of the organic matter, which may be derived from a variety of different sources, like

bacteria, phytoplankton, plant, algal community, humic terrigenous material and small contributions of aquatic fauna.

5.3 Silty siliceous mudstone facies (SSM)

Description:

The silty siliceous mudstone (SSM) facies is grey to dark grey in color and characterized by micaceous to slightly arenaceous mudstone to pure claystone with distinctive interlaminated quartzose siltstone laminae (0.2 to 3mm thick). Lower bedding contacts between siltstone laminations and mudstone are generally planar, whereas the upper bedding contacts occasionally fine-upwards to claystone (Fig. 11b). Individual grains within the siltstone laminations are very fine- to coarse silt-sized, angular to sub-angular shaped, and moderately to well-sorted. Minor siderite cement is locally present. Clay minerals include illite, mica, kaolinite, and chlorite, while accessory minerals include rutile, feldspar. The siltstone laminations are well cemented by quartz. The SSM facies is composed of ~50% quartz (both monocrystalline and polycrystalline) and 35% clay minerals. Concentrations of organic matter are visible within the mudstone/claystone intervals but are relatively low (1.0 to 1.5 %). There is low to moderate bioturbation. Visible porosity is ~1 -2%; primarily intergranular micro porosity associated with siderite, along with porosity associated with microfractures is observed (see Appendix-1). In general, the Murteree Shale yields a higher proportion of SSM facies than the Roseneath Formation. In both formations, the proportion of SSM increases towards the top of each formation. SSM is the most abundant facies present in the study area and represents about 25% of the lithofacies present in the Murteree Shale and 15% of lithofacies present in the Roseneath Shale.

Interpretation:

The highly interlaminated nature of SSM is the most diagnostic feature of this lithofacies and it represents the relatively high-energy facies in the study. This facies is interpreted to reflect a profundal lake setting. The SSM facies is coarser grained than other lithofacies in the Murteree and Roseneath formations and suggests deposition in a more proximal or higher energy setting than for the other three lithofacies. The lower clay content and organic content support both a higher energy setting and shallower, more oxygenated bottom waters. This facies is interpreted to represent deposition on the outer shelf associated with repeated storm activity, or more likely at the toe of a delta system in the prodelta depocenter and associated with repeated deposition of small-scale turbidites.

5.4 Calcareous siliceous mudstone facies (CSM)

Description:

CSM facies is also common in both the Roseneath and Murteree shales; characterized by massive, dark grey to black carbonate cemented mudstones with abundant siderite concretions. Euhedral to subhedral sparry calcite and concretionary siderite cements are the most distinctive feature of this facies. Minor to moderate amounts of terrigenous silt and fine-grained sand are present, mostly rounded to sub-rounded quartz and K-feldspar. Disseminated organic matter is low to moderately abundant (2.0%) (Appendix-1) and bioturbation is very common. Patchy microcrystalline carbonate mud and authigenic sparry calcite (sparite) represent ~1 to 2%, while siderite makes up ~50-60% of the cement present in CSM. Clays account for 35% and are composed of calcite–filled micro-fractures locally common in the Roseneath Shale (Figs. 12a-12b). Distinctive siderite concretions make up a large volume (10 to 25%) of this facies and are most common within the Murteree Shale (Figs. 12d and 12e). Porosity is visually estimated at approximately 2%, with most porosity being intergranular and intercrystalline micropores (Fig. 12d). In general, the Murteree Shale yields a higher proportion of CSM than the Roseneath Shale. Based on lithofacies, CSM represents about 15% of the Murteree and 10% of the Roseneath Shale.

Interpretation:

The high carbonate content is the most distinctive feature of the CSM, and it is likely to represent a near shore setting. It is interpreted to have been deposited on a relatively calm, shallow water setting on the basis of intense burrowing. Siderite appears approximately in all the units as rounded calcareous concretions and surrounding the detrital grains. These concretions formed during late diagenesis because of bed deformation during compaction, which occurs within siliceous calcareous mudstone facies. The concretion siderite was deposited in sediments formed later in burial history. In oxygen deficient depositional environmental hematite or pyrite is commonly transformed into siderite.

This facies by virtue of its digenetic overprint developed preferentially in more silty intervals. From core intersection, it is not possible to determine whether the cemented zones represent concretions or continuous horizons. The source of the carbonate is likewise uncertain. It is unlikely to have been generated from a lacustrine biogenic source. Albitisation of calcic plagioclase within the underlying sediment accumulation of the Cooper

Basin is the possible source. Limestone represented beneath the Cooper Basin is also a possibility.

In General, the Murteree Shale yields a higher proportion of (SM) than the Roseneath Shale does. In both shales, the proportion of SM increases towards the top of each formation. SM represents about 23% of the lithofacies present in the Murteree, whereas it only represents 12% of lithofacies present in the Roseneath. For the OSM the Murteree Shale yields a higher proportion of (OSM) than the Roseneath Shale. In both shales, the proportion of OSM increases towards the top of each shales. OSM represents about 4 to 5% of the lithofacies present in the Murteree, whereas it only represents 3 to 4% of lithofacies present in the Roseneath. The Murteree Shale yields a higher proportion of (SSM) than the Roseneath Shale. In both formations, the proportion of SSM increases towards the top of each formation. SSM represents about 25% of the lithofacies present in the Murteree, whereas it only represents 15% of lithofacies present in the Roseneath and yields a higher proportion of (CSM) than the Murteree Shale does. CSM represents about 15% of the lithofacies present in the Roseneath, whereas it only represents 10% of lithofacies present in the Murteree.

6. Electrofacies:

Electrofacies represent unique log responses that reflect petrophyical properties of rocks and formation fluids, and can be used for correlation purposes. Four distinct electrofacies A-D were identified for the Roseneath and Murteree shales in this study. Electro-facies were based on wireline log character and associations with lithofacies described from the core. Electrofacies are based on (GR) (DT) and (RHOB) logs responses from the two wells, Moomba-46 and Dirkala-02, and correspond to the respective lithofacies documented earlier. Cyclic facies stacking patterns are apparent from the logs. The same parameters were then applied to wells devoid of cores.

In order to build a relevant model that links lithofacies to their respective electrofacies, it is important to make a general classification of identified facies associations and assume that they are conformable both vertically and laterally. Gamma-ray logs measured from core reflect changes in lithofacies particularly well and hence provide excellent confirmation that the application of electrofacies provides a valuable approach for facies investigation in other parts of the basin, where wells have been logged, but not cored (Figs. 13-17).

6.1 Cluster Analysis:

Geostatistical analysis of predicted facies (e.g., Boyce et al., 2010; Lash et al., 2011) is based on conventional wireline data as presented in Figures 15 and 17. The cluster analysis links the wireline logs response to lithofacies recognized from the core. The attributes of electrofacies and their relationship to lithofacies are given in Table 3.

The aim of cluster analysis is to classify dataset into groups that are internally homogeneous and externally isolated on the basis of the measure of similarity or dissimilarity between groups. The cluster analysis can be compared with unsupervised classification, neither, dictated by an external model or determined by reference data set of objects whose identity is known beforehand. In cluster analysis, a firstly database of attribute measurements is compiled for the objects to be a cluster (Figs. 15 and 17).Then matrix of similarities or statistical distances between the objected is computed on the basis of the collective treatment of the attributes. The clustering algorithm is applied to the similarity matrix as an iterative process. The pairs of objects with the highest similarities are merged, the matrix is recomputed, and the procedure is repeated .Ultimately, all the objects are in one giant

cluster. The clusters are obtained by standard K-means algorithm that is used in the resultant clusters were then observed through dendrogram and final cluster were then calculated. The identified clusters were then assigned a facie type and the same logic facies were determined for the unknown well having all these curves in the (Table 3).

The electrofacies are compared with stratigraphic sections of the bored wells (Figs.15 and 17). For the electrofacies, modelling mineral composition and organic matter contents is essential. The modelling has integrated the core data from lithofacies analysis and extrapolated across both shale formations. GR and density logs are used to predict TOC content in shale (Schmoker, 1981; Fertl et al., 1988) and sonic log value is decreased by low organic matter to its lower acoustic velocity (Passey et al., 1990).

6.2.1 Electrofacies A:

Electrofacies A is used to describe the characteristic log response observed for the siliceous mudstone lithofacies. The thickness of this electrofacies varies in thickness from 2 to 10m and is usually characterized by blocky and fining upward response. The gamma ray intensity picks out intervals that are siliceous -rich. In particular, siliceous mudstone is indicated by low to the moderate gamma-ray signature, while sonic log response show curve with slightly increasing. This electrofacies association mostly appears in Roseneath Shale Moomba-46 well (Fig.14) at various depths in the range of 8080m, 8100m, 8120m and 81240m and is usually characterized by GR >150 API units. Similarly, for the Murteree Shale in the Dirkala-2 well (Fig.16), it is observed at depths of 1890m, 1892m, 1908 m, 1921m, 1932m-1938m and is characterized by GR>150 API units. The sonic signatures are moderate 65 µs/f units. Electrofacies A is the most common observed facies in both shales and interlayered between B, C and D electrofacies.

6.2.2 Electrofacies B:

Electrofacies B is used to describe the characteristic log response observed for the organic silicious mudstone lithofacies and reflects the higher abundance of organic content. The profile of this interval is showed by core section and log. Gamma ray log enabling qualitative identification of organics material. The variation of this facies is also quite stable. High gamma ray reflection (API >200) trend indicates that this unit contains elevated organics and/or radioactive clay minerals (possibly slightly elevated amounts of elements such as U, K, etc). This is characterized by apparent coarsening upward trends. Gamma-ray

log response is very high, mostly increasing upward, while the sonic response is very low. Electrofacies B is the second most abundant electrofacies, varying in thickness from 2 to 6 m. The electrofacies mostly appears in the Roseneath Shale between 2464m to 2478m in Moomba-46 well. The shales there have GR > 200 API units. In the Murteree Shale, Electrofacies B is observed between 1892m to 1936m in the Dirkala-2 well and is characterized by GR> 180 API units. The sonic signatures are moderate 40 µs/f units.

6.2.3 Electrofacies C:

Electrofacies C is used to describe the characteristic log response observed for the silty siliceous mudstone facies. The electrofacies association with the SSM is interpreted based on the low gamma signatures and Sonic, density etc values than facies A or B. Overall, the silty siliceous mudstone yields gamma-ray and sonic signatures that are moderate. This facies thickness varies between 2 to 8m. It occurs in the Roseneath Shale core section between 2470m to 2478m in the Moomba-46 well, where GR> 190 API units are observed. In the Murteree Shale, the core section between 1901m to 1916m (Dirkala-2) has some of these facies where GR>160 API units are observed. The sonic signatures are moderate 60 µs/f units.

6.2.4 Electrofacies D:

Electrofacies D has the lowest GR counts of 100-120 API of all facies combined with a sonic signature of ~75 µs/f units. Density logs used to describe the characteristic log response observed for the calcareous siliceous mudstone. The gamma ray response shows the decrease in reading, but this may not be inaccuracy rather an indication of non-radioactive pore filling cement, such as siderite, calcite. The sharp decrease in gamma-ray log response for this facies show a very low gamma ray as compare to Electrofacies A. The thickness of this facies varies 2 to 6m. This facies is observed at around 2472m depth in the Mooba-46 well (Roseneath Shale) and between 1892-1938m of the Dirkala-2 (Murteree Shale). The log reading is characterized by GR 100 to 120 API units, while sonic signatures are moderate 75 µs/f units.

7. Discussion

The analysis of shale mineralogical compositions (Tables 1-2), and their correlation with core gamma-ray log, integrated with the geochemical dataset (Appendix-1) allows a synthesis of the shale reservoir characteristics in the Roseneath and Murteree shales. In this case, two key minerals, quartz, and siderite, can be assessed in terms of their implications for the reservoir quality of the shales. Quartz shows a considerable compositional range with significant variations for brittleness of the Roseneath and Murteree shales. Large silica filled in the form of Polycrystalline and angular to sub-angular grain shapes. A substantial proportion of the quartz grains are polycrystalline in both shales. (Figs.9b-9f). These types of quartz concentrated in lag deposits on erosion surfaces and sequence boundaries. Even though these polycrystalline quartz grains constitute less than 1% of the deposited sediment volume, they are important for the primary porosity and reconstructing the depositional history of mudstone.

Most previous studies show the formation of polycrystalline quartz focused on the bulk transformation rate between silica polymorph and polycrystalline may occur in a variety of siliceous shale have been frequently found in the sedimentary basin (Mosen folder & Bohlen, 1997; Hinman, 1998). These siliceous sediments, polycrystalline quartz formation and growth rate formation via series of transformation from opal to polycrystalline (Mizutani, 1976). According to William et al., 1985 and Azarousal et al., 1997 the fine grained polycrystalline quartz is commonly at high nucleation rate with relatively slow growth rate. Siliceous sediments favor the high nucleation rate for the formation of polycrystalline quartz and quartz varies with temperature and pressure. Detrital silt quartz where quartz grains are essentially uniform, while polycrystalline quartz shows the irregular shape and this type indicates the low porosity in shale reservoir see in (Fig.9).

The genesis of siderite in both shales has been a matter of discussion. Siderite may be interpreted to the hydrothermal metasomatic recrystallization of carbonate rock. Fe-bearing solution may have been mobilized during the catagenesis of the lower basement rocks. The solution may have migrated into carbonate during tectonic activity of the region and the input of solutions led to the local recrystallization of primary carbonate rock and the formation of new Mg-Fe carbonates. On the other hand, siderite concentrations have been observed to more or less restricting along what would have been preferential migration pathways for pore water eliminated during compaction. It seems that this concretionary siderite may be grown from pore water migrating down a pressure gradient and maintaining the condition of slight super saturation with

respect to carbonates. This first formed carbonate and the concretion centre precipitated from pore solutions rich in iron with low activity of calcium and magnesium. As growth proceeded with its burial and compaction there may have been a systematic decrease of Fe and calcium became more abundant. The majority of the carbonate precipitated early and the growth of the later carbonate almost certainly would have spanned a lengthy interval up to more or less complete sediment compaction.

The late diagenetic formation of siderite plays an important role for secondary porosity and improved fracability, but also increase the total porosity (Ahmad, 2014). Concretionary siderite is quite common in the Roseneath and Murteree shales, the implication of siderite is not favourable for the density tool in the oil and gas industry. The litho-density log is a new form of the formation density log and siderite Feco3 affects the density tool showing the cycle skipping leading to incorrect porosity (Glover, 2010).

A perfect model should integrate the entire conventional well and core data and up-scale lithofacies from core scale to well-scale and finally to regional scale. The electrofacies model is to look at the typical wireline log response between data points in the multivariate space of logs, in order to group them into classes and each class represents the different electrofacies (Euzen et al., 2010).

The uncertainty of the proposed electrofacies models of shales depends on the primarily available input data and associated primary interpretation of core data. The core-defined lithofacies, which is an associated suit of borehole conventional logs, and the selection of data generated realization using the same neural network model resulted in the variation of the lithofacies proportions. Reference is the important role to evaluate the precision of generated realizations. However, the overall ability of the predicted lithofacies models using soft data sets, different computed models, and various scales provides some confidence that those models seem to have validity. The validity of the model come from matching with the core data.

Porosity in the Roseneath and Murteree shales is rarely observed and consists of matrix-hosted micro porosity. From SEM and thin section studies, and petrophysics (Figs. 20-22) the visible porosity is estimated and it varies between 1 to 6%. The natural fractures and micro-fractures in these shales are completely healed by secondary calcite and other mineral cement. These are prevented by the preservation of the natural fracture porosity. The most common pore type is approximately <0.005 mm in both shales. On the other hand, matrix and micro-porosity are also

observed in the thin section as tiny pinpoints throughout the detrital matrix. In many cases, the individual pore sizes <2 microns are too small to resolve under the petrographic microscope. The intragranular microcracks present at different sites of grain-to-grain contact, where compaction stresses are concentrated and fracture apertures are extremely narrow while secondary intergranular pores represent voids that were filled with carbonate cement and diagenetic dissolution in both shales.

7.1 Distribution of Facies

The preliminary results of this study suggest the use of well log cluster analysis and electrofacies probabilities may provide a simple and effective way of integrating quantitative data derived from the core from conventional well data. The technique of lithofacies may be used to quantify facies between cored intervals or in neighbouring wells where core has not been undertaken. A careful normalization of logs must be done in order minimize Variation related (Fig. 18).

The distribution provides an adequate exploration for the basin ward extension of channelized features of Nappameri, Allunga, Tenappera troughs and for the occurrence of four lithofacies siliceous mudstone, organic siliceous mudstone, silty siliceous mudstone. Consequently facies analysis derived from electrofacies. The regional scale having the largest electrofacies that describes lithofacies suggest that Nappameri to Tenappera troughs would be the suitable location to evaluate Roseneath and Murteree shales and fairways to help this work could perhaps extend to across the basin succession where siliceous mudstone lithofacies has been identified a major dominant facies across the basin.

Petrophysical characterization of the lacustrine sediments succession, sedimentary facies logs of the Roseneath and Murtree shales, comparison with Big lake-70, Moomba-46, Encounter-01 Dirkala-02. (Figs. 19-21). Shale volume was evaluated using the GR through the application of log data, minimum and maximum values within clean sands and shales. The volume of the shale was estimated GR, neutron density log combination. The geophysical resistivity log shows pronounced peaks in the bedrock and it is fairly constant with only very small peak throughout the entire lacustrine section, exhibiting some smaller but smooth shifts both Roseneath and Murteree shales. Resistivity curves point at a rather uniform succession of sediments without abrupt changes even though the sediments are highly variable and change rapidly between homogeneous and

laminated layers and mass movement deposits. This is reflected in the fact that almost the entire lacustrine succession is represented in Roseneath and Murteree shales.

7.2 Depositional Model

Seismic events were mapped over the Innaminka Dome structure and tied into the Encounter-1 well (gamma ray log). In a depositional model based on these data the wide shelf at the North-South part of the depositional model (Fig.22) is characterized by aggrading sequences; seismic data from the south and north-south shelf seismic profile of cooper Basin, seismic traverse (North-South) from the Innaminka Dome to proposed Encounter-01 showing to be down dip and outside structural closure at Roseneath level 2D seismic lines. Lacustrine intervals of the Murteree and Roseath shales are characterized by the seismic velocity of 2120ms and Murteree 2,250ms and a thickness of about Roseneath 194.2m, Murteree shale 79m. The Roseneath comprises lacustrine sediments overlying the Epsilon Formation. The gamma ray log measure natural radioactivity in formations, therefore enabling qualitative identification of zones of shale high gamma readings from sand low gamma readings. These are identified from abrupt changes in the gamma ray log. The stratigraphic intervals of R1, R2, R3 are inferred based on the seismic reflectors. The sedimentary package appears a series of prograding reflectors on a marginal slope overlain by subparallel laterally continuous beds. The depositional environment is interpreted as lacustrine. All reflectors are dominantly lacustrine succession based on the laterally continuous reflector and spiky log. The irregular gamma-ray log trend is interpreted to represent shales beds. The high amplitude reflectors support this. The overall trend appears to be a depositional lake. The GR log trend clearly shows the spiky log trend. The sharp boundaries with an overlying and overlying sequence in a plane the existence of abrupt change Roseneath, Epsilon, and Murteree. The Epsilon a low gamma coarse-grained unto a higher gamma coarse-grained unto a higher gamma finer unit of Roseneath and Murteree shales.

The REM are identified from abrupt changes in the gamma ray log. The Roseneath, R1 and Murteree,R3 have been separated into members based on these sharp changes in gamma counts. There is an excellent correlation between the high amplitude seismic events. In Epsilon, R2, gamma ray value increase systematically then decrease in the same manner. The log characteristic of follows a bow trend. The sharp based sequence represents a significant change in depositional environment (Fig. 22). The overall log trend is very irregular and the spike of logs suggest due to rapidly alteration lithology. This either reflects a multitude of discrete depositional events or variable sediment supply.

7.3 Comparison with the North American shale gas

In the evaluation of the hydrocarbon resource system, it is important to understand the various lithofacies characteristics associated with shale gas. The unconventional shale gas plays in the United States: the Cretaceous Eagle Ford Shale in southwest Texas, the Upper Jurassic Bossier and Haynesville shales from northwest Lousiana, the Devonian Marcellus Shale, Appalachian Basin and the Missippian Barnett Shale from north Texas. These formations are composed largely of clays, quartz, carbonate, organic matter, with accessories minerals of feldspar, mica, pyrite and sulfate minerals. The Eagle Ford Shale a marl, containing biogenic carbonate and minor biosiliceous material (Ozkan et al., 2013).The Haynesville and Bossier shales contain much less carbonate, with high proportions of quartz and clay minerals(Cicero et al., 2010).

Barnett Shale is unusually quartz-rich due to a high content of biogenic silica, In detail it has five major lithofacies: 1) black shale, 2) calcareous black shale, 3) lime grain stone, 4) dolomite black shale, and 5) phosphatic black shale (Henk et al., 2000, Henk 2005; Hicky et al., 2006; Louck and Ruppel, 2007). All these lithofacies have high gamma ray signatures > 100 API. The highest reflection of gamma-ray is encountered in Phosphatic black shale. The Barnett Shale petrographic study shows the presence of pyrite, scattered calcite shell fragments, conodonts and Tasmanite algal fragments (Flippin, 1982).The Roseneath and Murteree shales of the Cooper Basin with high rich quartz and clay minerals contents represent comparable lithologies(Table 4). The presence of carbonate cement in the Cooper Basin units is a difference. How such rocks may respond to fracking remains to be tested.

Deposition environment of Barnett Shale is deep water basin with poor, circulation stratified water column, marine upwelling contributed to algal blooms, water depth perhaps 500 - 650 ft, while Marcellous Shale is deep water basin with poor circulation stratified water column. And anoxic bottom water, marine upwelling contributed to algal bloom water depth perhaps 300- 1000ft (Kathy, 2011).By comparison with Roseneath and Murteree shales wave ripple suggested possible storm reworking. Loadmarks, flame structure and slump indicate mass flow set slope instability. A lacustrine environment of deposition is interpreted for the Roseneath Shale, water depth 200-500 ft.The Murteree Shale was deposited in a large, relatively deep, fresh water lake, depth 300-600 ft with occasional dropstone indicating seasonal ice flow. (Gravestock et al,1995).

8. Conclusions

- Roseneath and Murteree shales are highly heterogeneous formations. Four distinct lithofacies were identified; siliceous mudstone, organic siliceous mudstone, silty siliceous mudstone and calcareous siliceous mudstone. The siliceous mudstone and organic siliceous mudstone are the most dominant lithofacies.

- Roseneath and Murteree lithofacies can be defined from core and wireline logs in terms of mineral composition, clay percentage, and organic matter, the ratio of quartz, carbonate, and TOC content. These are the six key criteria for recognizing the Roseneath and Murteree shales mudstone lithofacies.

- A lacustrine model for the deposition of the shales suggests that they were deposited below the storm-wave base. The organic matter indicates the Roseneath and Murteree shales were generally anoxic of the lake bottom that had been aerobic. In an aerobic setting, bioturbation is common. Both shales have high, intense burrowing indication that was likely deposited in a calm and relatively low stressed and slow current deposition. The facies of both shales also represent the high and low energy activity of the lakes levels.

- The results were combined with four electrofacies classifications to produce four general facies associations as an input to reconstruct the facies within the Roseneath and Murteree shales. Organic matter is more abundant in the Roseneath and Murteree shales and shows potential shale gas reservoirs. The reservoir characteristics are based on petrographic studies specifically for Quartz, clay, and carbonates showing good reservoir conditions.

Acknowledgement: Quaid Khan Jadoon would like to acknowledge for his Ph.D. funding provided by the Graduate Research School (GRS) Support Program at the Department of Geosciences, College of Science Technology & Engineering at James Cook University Queensland Australia. DMITRE (Department for Manufacturing, Innovation, Trade, Resources and Energy, Government of South Australia) generously provided core samples for this study. Quaid Khan is grateful for the technical services rendered by Trican Geological Solutions Ltd Calgary, Alberta, Canada, in respect to the XRD data. Quaid Khan also acknowledges Prince Owusu Agyemang and colleagues of sedimentology research group (Gravel Monkeys) at JCU and Assistant Geologist Fawahid A.K Jadoon (Comsat). Senior Technical advisor and Team Lead Tahir M. Khan (LMKR). Special thanks to Syed Anjum Shah Chief Geologist Saif Energy Islamabad for his useful guidance.

9. References

Ahmad,M. 2015 Petrophysics and mineralogical Evaluation of Shale gas reservoirs (A Cooper Basin Case study) .

Alberta Geological Survey, http://www.ags.gov.ab.ca/energy/shale-gas/shale-gas.html [June 10, 2012].

Alexander, E.M. and Hibburt, J.E. (Eds), 1996. The petroleum geology of South Australia. Vol. 2: Eromanga Basin. South Australia. Department of Primary Industries and Resources. Petroleum Geology of South Australia Series.

Alexander, E.M. and Krieg, G.W., 1995. Stratigraphy — lower non-marine succession. In: Drexel, J.F. and Preiss, W.V. (Eds), the geology of South Australia. Vol. 2, The Phanerozoic. South Australia. Department of Mines and Energy. Bulletin, 54:105-111.

Alexander, R., Larcher, A.V., Kagi, R.I. and Price, P.L., 1988. The use of plant-derived biomarkers for correlation oils with source rocks in the Cooper/Eromanga Basin system, Australia. APEA Journal, 28(1):310-324.

Ashley, G.M., Shaw, J. and Smith, N.D., 1985. Glacial sedimentary environments. Society of Economic Paleontologists and Mineralogists. Short Course, 16:246.

Azaroual, M., Fouillac, C., Matray, J.M. (1997): Solubility of silica polymorphs in electrolyte solutions; II, Activity of aqueous silica and solid polymorphs in deep solutions from the sedi- mentary Paris Basin. Chemical Geol., 140, 167-179.

Battersby, DG.,1977-Cooper Basin gas and oil fields.In:Leslie,R.B., Evans, H.J., & Knight,C.L.,(eds), Economic Geology of Australia and papua New Guinea, 3, Petroleum Australian Institute of Mining and Metallurgy, Parkville.

Boreham.C.J. and Summins. RE., 1999- New insights into the active petroleum systems in the Cooper and Eromanga basins, Australia. APPEA Journal, 39 (1), 263–96.

Boyce, M. L., and T. R. Carr, 2010, Stratigraphy and petro-physics of the Middle Devonian black shale interval in West Virginia and southwest Pennsylvania: AAPG Search and Discovery article 10265, accessed May 22, 2013, http://www.searchanddiscovery.com/documents/2010 /10265boyce/poster01.pdf.

Boucher, R.K., 2000. Analysis of seals of the Roseneath and Murteree Shales, Cooper Basin, South Australia. South Australian Department of Primary Industries and Resources. Report Book 2001/015.

Brett, C. E., and G. C. Baird, 1996, Middle Devonian sedi-mentary cycles and sequences in the northern Appala-chian Basin: Geological Society of America Special Pa-per 306, p. 213–241.

Bruner.R.K & Smosna, K. R. (2011, April). A Comparative Study of the Mississippian Barnett Shale, Fort Worth Basin, and Devonian Marcellus Shale, Appalachian Basin. *U.S. Department of Energy*.

Chaney, A.J., 1998 Gondwana glaciation : Merrimmelia Formation, Cooper Basin South Audtralia, Australia*. Aberdeen Uneiversity. Ph.D. thesis* (unpublished)

Crowell, J.C. and Frakes, L.A., 1971. Late Paleozoic glaciation of Australia. *Geological Socity of Australia. Journal*, 17(2):115-155.

Cramer, D.D. (2008): stimulating unconventional reservoirs: lessons learned, successful practices, area for improvement; 2008 Unconventional Gas Conference, Keystone, February 10-12, 2008 society of Geologists.

Deutsch, C. V., 2002, Geostatistical reservoir modeling: New York, Oxford University Press, 376 p.

Euzen, T., E. Delamaide, T. Feuchtwanger, and K.D. Kingsmith, 2010 Well Log Cluster Analysis: An Innovative Tool for Unconventional E xploration, in CSUG/SPE 137822, Canadian Unconventional Resources and Int ernational Petroleum Conference, Calgary, Alberta, Canada, 19 – 21 October 2010.

Fournier, F., 1997 , Méthode statistique de classements d'évènements liés aux propriétés physiques d'un milieu complexe tel que le sous sol. Brevet EN 97/12.182 N°2.768.818 (France 22/09/97), brevet US n°6.052651 (USA, 21/09/98).

Flippin, J.W., 1982, The stratigraphy, structure, and economic aspects of the Paleozoic strata in Erath County, North-Central Texas, in Martin, C.A., ed., Petroleum geology of the Fort Worth Basin and Bend Arch area: Dallas Geological Society, p. 129–155.

Fairburn, W.A., 1992. Geometry of reservoir trends in the Epsilon Formation sands, southern Cooper Basin, South Australia. APEA Journal, 32:339-358.

Falivene, O., P. Arbues, A. Gardiner, G. Pickup, J. A. Munoz, and L. Cabrera, 2006, Best practice stochastic facies modeling from a channel-fill turbidite sandstone analog (the Quarry outcrop, Eocene Ainsa Basin, northeast Spain): AAPG Bulletin, v. 90, no. 7, p. 1003–1029, doi:10.1306 /02070605112.

Fielding, CR., Frank, T.D., Birgenheir, L.P.,Rygel, M.C., Jones, A.T., Roberts, J., 2008a. Stratigraphic imprint of the Late Paleozoic Ice Age in eastern Australia:a record of alternating glacial and nonglacial climate regime. Journal of the Geological Society of London 165, 129-140.

Fielding, CR., Frank, T.D.,Isbell,J.L.,2008b. The late Paleozoic ice age- a review of current understanding and synthesis of global climate patterns.In: Fielding, C.R., Frank, T.D., Isbell, J.L.,(Eds.), Resolving the Late Paleozoic Ice Age in Time and space: Geological Society of America Special publication, 441. Boulder, CO.

Gravestock, D.I. and Morton, J.G.G, 1984. Geology of the della Field, a prespective on the history of the Cooper Basin. APEA Journal, 24:266-277.

Gravestock, D.I, Hibburt, J.E., Drexel, J.F. (Eds), The Petroleum Geology of South Australia, Vol. 4: Cooper Basin. South Australian Department of Primary Industries and Resources. Report Book 98/9:129-142.

Glover, P. (2010). Measurements of the photo-electric absorption (PEF) litho-density log for common lithologies. Petrophysics MSc Course Notes the lithodensity Log, pp 146.

Gravestock et al., 1995. STRZELRCKI, South Australia, sheet SH54-2, South Australia. Geological Survey. 1:250 000 Series- Explanatory Notes.

Gatehouse, C.G., 1972-Formations of the Gidgealpa Group in the Cooper Basin. Australasian Oil & Gas Review 18:12, 10-15.

Galli, A., Beucher, H., Le Loc'h, G., Doliguez, Group, H., 1994. The pros and cons of the truncated Gaussian method. In: Armstrong, M., Dowd, P.A. (eds.). Geostatistical Simulations. The Netherlands, Kluwer Academic Publishers, 217-233

Gilby, A.R. and Foster, C.B., 1988. Early Permian palynology of the Arckaringa Basin, South Australia. Palaeontographica. Abteilung B: Palaeophytologie, 209(4-6):167-191.

Gostin, V.A., 1973. Lithologic study of the Tirrawarra Sandstone based on cores from the Tirrawarra Field. Report for Delhi International Oil Corporation (unpublished).

Haldorsen, H. H., and D. M. Chang, 1986, Notes on stochas-tic shales: From outcrop to simulation model, in L. W. Lake and H. B. Caroll, eds., Reservoir characterization: New York, Academic Press, p. 445–485.

Henk,F., 2005, Lithofacies of the Barnett Shale Formation from outcrop to subsurface (abs): Barnett Shale Symposium III, Ellison Miles Geotechnology Institute: Texas Petroleum Technology Transfer Council, Texas Petroleum Technology Transfer Council, Texas Region, CD-ROM.

Henk,F., J.T.Breyer, and D.M. Jarvie, 2000, Lithofacies, petrography, and geochemistry of the Barnett Shale outcrop geochemistry (ab), in L.Brogdon, ed., Barnett Shale Symposium, Fort Worth, Texas: Oil Information Library of Fort Worth, Texas, p.7.

Hill, A.J., 1995. Source rock distribution and maturity modelling. In: Morton, J.G.G. and Drexel, J.F. (Eds), The petroleum geology of South Australia. Volume 1: Otway Basin. South Australia. Department of Mines and Energy Report Book, 95/12:103-125.

Hickey,J., and F.Henk, 2006. Barnett Shale, Fort Worth Basin:Lithofacies and implications(abs):AAPG Southwestsection.org/SWSAAPG2006,Midland,Texas,http://www.southwestsection.org/SWSAAPG2006/Convention2.htm(accessed October 15, 2006).

Hickey, J. J., and B. Henk, 2007, Lithofacies summary of the Mississippian Barnett Shale, Mitchell 2 T.P. Sims Well, WiseCounty, Texas:AAPGBulletin, v. 91, no. 4, p. 437– 443, doi:10.1306/12040606053.

Hinman, N.W. (1998): Sequence of silica phase transitions; effects of Na, Mg, K, Al and Fe ions. Marine Geol., 147, 13-24.

Jadoon, Q.K., Roberts. E., Blenkinsop, T., Wüst, R.A.J.2016 Organic petrography and thermal maturity of the Permian Roseneath and Murteree shales in the Cooper Basin, Australia, Int. J. Coal Geol., http://dx.doi.org/10.1016/j.coal.2016.01.005.

Loucks, R.G., and Ruppel, S.C., 2007, Mississippian Barnett Shale: lithofacies and depositional setting of a deep-water shale-gas succession in the Fort Worth Basin, Texas: American Association Petroleum Geologists Bulletin, v. 91, p. 579–601.

Lash, G. G., and T. Engelder, 2011, Thickness trends and se-quence stratigraphy of the Middle Devonian Marcellus Formation, Appalachian Basin: Implications for Acadian foreland basin evolution: AAPG Bulletin, v. 95, no. 1.

Mizutani, S. (1966): Transformations of silica under hydrothermal conditions. Nagoya Univ. J. Earth Sci., 14, 56-88.(1970): Silica minerals in the early stage of diagenesis. Sedimentology, 15, 419-436.

Morton, J.G.G., 1983. The geology and reserves of the Toolachee Field, Cooper Basin, South Australia. South Australia. Department of Mines and Energy. Report Book, 827.

Mosenfelder, J.L. & Bohlen, S.R. (1997): Kinetics of the coesite to quartz transformation. Earth Planet. Sci. Letters, 153, 133-147.

Myers, R. (2008). Marcellus shale update, Independent Oil & Gas Association of West Virginia.

O'Brien, N., and R.M. Slatt, 1990, Argillaceous Rock Atlas, Springer-Verlag, N.Y., 141 p

PIRSA, 2012 http://www.pir.sa.gov.au/data/assets/pdf.file/0003/33663/prospectivity Cooper.pdf.

Kathy R. Bruner and Richard Smosna, 2011, A Comparative Study of the Mississippian Barnett Shale, Fort Worth Basin, and Devonian Marcellus Shale, Appalachian Basin, US Department of Energy, DOE/NETL - 2011/1478.

Kapel, A.J., 1972. The geology of the Patchawarra area, Cooper Basin. APEA Journal, 6:71-7.

Klemme, H.D., 1980 - Petroleum basins- classifications and characteristics. Journal of petroleum geology vol.3, pp. 187-207.

Passey, Q. R., S. Creaney, J. B. Kulla, F. J. Moretti and J. D. Stroud, 1990, A practical model for organic richness from porosity and resistivity logs: AAPG Bulletin, V. 74, P 1777-1794.

Price, P.L., Filatoff, J., Williams, A>J., Pickering, S.A., & Wood, G.R., 1985- Late Paleozoic and Mesozoic palynostratigraphic units, CSR Ltd: Oil & Gas Division. Unpublished company report 274/25.

Stuart, W.J., 1976. The genesis of Permian and Lower Triassic reservoir sandstones during phases of southern Cooper Basin.

Schlumberger, 2011, accessed July 20, 2015, http://www.slb.com/services/software/geo/petrel/geomodeling/facies_modeling.aspx.

Taylor, S., Solomon, G., Tupper, N., Evanochko, J., Horton, G., Waldeck, R. and Phillips, S., 1991. Flank plays and faulted basement: new directions for the Cooper Basin. APEA Journal, 31(1):56-73.

Timofeev, P.P., and Bogolyubova, L.I., 1981. Cretaceous sapropelic deposits of Deep Sea Drilling Project Sites 463,465, and 466. In Thiede, J., Vallier, T.L., et al., Init. Repts. DSDP, 62: Washington (U.S. Govt. Printing Office), 891-901.Wopfner, H., 1972-Depositional history and tectonics of South Australian sedimentary basins. South Australian Mineral Resources Review 113, 32-50.

Thornton, R.C.N., 1979. Regional stratigraphic analysis of the Gidgealpa Group, southern Cooper Basin, Australia. South Australia. Geological Survey. Bulletin, 49.

Veevers, J.J. and Powell, C.McA., 1987. Late Palaeozoic glacial episodes in Gondwanaland ref lected. In: Transgressive–regressive depositional sequences in Euramerica. Geological Society of America. Bulletin, 98:475-487.

Waples, D.W., 1980. Time and temperature in petroleum formation: application of Lopatin's method to petroleum exploration. Am. Assoc. Pet. Geol. Bull. 64, 916–926.

Wopfner, H., 1972-Depositional history and tectonics of South Australian sedimentary basins. South Australian Mineral Resources Review 113, 32-50.

Williams, B.P.J., Wild, E.K., & Suttill, R.J., 1985-Paraglacial aeolianites: Potential new hydrocarbon reservoirs, Gidgealpa Group, southern Cooper Basin.The APEA journal 25:1, 291-310.

Williams, P.F.V., and A.G. Douglas.1983.A preliminary organic chemistry investigation of the Kimmeridgian oil shales. In A.G. Douglas and J.R. Maxwell (eds.), Advances in organic geochemistry 1979, Oxford: Pergamon Press, pp.531-545.

Williams, B.P.J., Wild, E.K., & Suttill, R.J., 1985-Paraglacial aeolianites: Potential new hydrocarbon reservoirs, Gidgealpa Group, southern Cooper Basin. The APEA journal 25:1, 291-310.

Williams, L.A., Parks, G.A., Crerar, D.A. (1985): Silica diagenesis, I. Solubility controls. J. Sed. Petrol., 55, 301-311.

Williams, B.P.J., 1995. Core workshop – 'non-marine deposystem'. Sagasco Resources Ltd (unpublished).

Wüst, R.A.J., Hill., Jadoon, Q.k., Nassichuk, and Alexander, 2015, Permian Lacustrine Unconventional Shales as Hyrocarbon Targets in the Cooper Basin, Australia: Rock Characteristics and Well and Production Challenges Feb 2015 (Applied Geoscience Conference-Houston Geological Society (USA).

Zhang, R.Y. & Lou, J.G. (1996): Coesite inclusions in dolomite from eclogite in the southern Dabie Mountains, China: The significance of carbonate minerals in UHPM rocks. Am. Mineral., 81, 181-186

Depth (m)	Quartz	Feldspars	Fe-carbonates	Ti-Oxides		Mica/clay minerals			TOC
		Albite	Siderite*	Rutile	Anatase	Muscovite	Illite	Kaolinite	
2462.7-2462.8	51.3	0.9	1.2	0.1	0.5	15.6	6.8	21.6	2.0
2463-2463.1	45.9	1.9	2.0	0.1	0.9	18.5	9.0	20.3	1.5
2463.3-2463.4	42.6	2.2	1.7	0.1	0.8	22.1	10.4	19.1	1.0
2463.5-2463.6	40.8	3.0	2.3	0.1	0.9	21.1	10.0	19.3	2.5
2463.7-2463.8	36.3	1.0	12.2	0.1	0.3	27.4	6.3	15.0	1.5
2464.2-2464.3	36.8	0.8	7.4	0.1	0.3	30.2	7.0	15.4	2.0
2464.6-2464.7	40.5	0.7	1.6	0.1	0.8	32.0	7.0	15.3	2.0
2464.7-2464.8	37.2	0.6	1.4	0.1	0.5	43.6	1.5	14.2	1.0
2465- 2465.1	39.9	0.9	1.8	0.1	0.8	43.1	2.5	9.0	1.9
2456.4-2465.5	33.4	0.7	6.9	0.1	0.3	42.0	3.0	12.6	1.0
2465.9- 2466	34.9	0.8	2.7	0.1	0.5	43.6	3.9	12.6	1.0
2466.7-2466.8	39.7	0.4	3.8	0.1	0.5	36.4	5.2	13.0	1.0
2466.9- 2467	36.4	0.2	3.5	0.1	0.6	34.7	6.0	16.6	2.0
2466.3-2467.4	43.3	1.9	4.4	0.1	0.9	25.4	7.1	15.0	2.0
2467.6-2467.7	43.0	1.5	3.5	0.1	0.9	29.0	5.9	14.7	1.5
2468 -2468.2	36.4	1.5	12.8	0.1	0.6	29.8	3.1	13.8	2.0
2468.4-2468.5	34.2	1.1	13.3	0.1	0.5	31.0	4.0	14.4	1.4
2470-2470.1	44.9	1.5	3.1	0.1	0.9	30.0	5.6	12.7	1.3
2475-2475.1	18.0	1.1	49.2	0.1	0.1	18.0	0.7	10.0	3.0
2476-2476.1	31.3	0.3	9.1	0.1	0.1	39.5	3.2	13.1	3.5

Table-1: Roseneath Shale mineral composition Moomba 46 well

Depth (m)	Quartz	Feldspars	Fe-carbonates	Ti-Oxides		Mica/clay minerals			TOC
		Albite	Siderite*	Rutile	Anatase	Muscovite	Illite	Kaolinite	
1892.81	48.3	0.9	3.7	0.1	0.6	23.2	8.9	12.4	2.0
1892.83	42.7	0.7	5.4	0.1	0.7	26.2	9.5	13.3	1.8
1892.808	40.1	1.2	11.7	0.1	0.6	13.1	18.3	12.5	2.5
1893.113	40.9	0.9	11.2	0.1	0.5	23.2	9.0	12.3	2.0
1893.6	38.9	0.8	4.4	0.1	0.5	37.6	4.5	12.3	1.0
1894.2	30.4	0.1	18.5	0.1	0.1	40.4	1.4	9.4	1.0
1895	58.0	1.1	4.4	0.1	0.7	8.8	8.3	14.8	4.5
1895.551	31.4	0.4	28.6	0.1	0.1	20.3	8.3	8.9	2.0
1895.660	27.4	0.1	31.0	0.1	0.1	29.2	0.1	10.4	2.5
1895.770	40.9	0.9	9.2	0.1	0.5	22.3	13.4	12.8	1.5
1896.161	45.6	0.9	1.0	0.1	0.6	23.2	13.2	13.1	3.5
1896	46.2	0.9	1.9	0.1	0.8	25.2	9.0	14.0	2.0
1896.2	46.8	1.3	3.0	0.1	1.2	20.8	7.8	16.0	3.0

Table-2: Murteree Shale mineral composition Dirkala-02 well

Electrofacies	Matching lithofacies siliceous mudstone	RHOB Density	DT Sonic	GR Gamma-ray
A	Siliceous mudstone	2.2 – 2.4 G/C^3	65 µs/f	150 API
B	Organic-siliceous mudstone	2.5 – 2.7 G/C^3	40 µs/f	> 200 API
C	Silty-siliceous mudstone	2.1-2.2 G/C^3	60 µs/f	190 API
D	Calcareous siliceous mudstone	1-2 G/C^3	75 µs/f	160 API

Table 3: Attributes of electrofacies and their relationship to lithofacies are given in the table

Shale	Basin	Age	Basin type	TOC	Depth	Environment of deposition	Mineral composition
Barnett	Fort Worth	Mississippian	Foreland	1-10%	2000-2800 m	Marine	35–50% quartz, 27% illite with minor smectite, 8–19% calcite and dolomite, 7% feldspars, 5% organic matter, 5% pyrite, 3% siderite, and traces of native copper and phosphate material
Marcellus Shale	Appalachian	Devonian	Foreland	2-6%	1500-2500m	Marine	27–31% quartz, 9–34% illite, 1–7% mixed- layer clays, 0–4% chlorite, 3–48% calcite, 0–10% dolomite, 0–4% sodium feldspar, 5–13% pyrite, and 0–6% gypsum.
Eagle Ford	East Texas	Late - Cretaceous	Passive margin	2-12%	1200- 4250m	Shallow marine	47% calcite, 11%quartz,3% pyrite, 25% illite, 17% kaolinite, 14% Albite, 3% dolomite, 19%muscovite.
Roseneath	Cooper	Permo-Triassic	Intracratonic	2-30%	1600- 2000 m	Lacustrine	30-45% quartz, 10-20% siderite, 1% rutile, 20-30% muscovite, 10-15% illite, 10-15% kaolinite
Murteree	Cooper	Permo-Triassic	Intracratonic	2-6%	1800 – 2200 m	Lacustrine	30-55% quartz, 10-25% siderite, 1% rutile, 20-35% muscovite, 10% illite, 15% kaolinite

Table 4: Generalized characteristics of productive American shales gas (Bruner & Smosna, 2011) and Cooper's shales(Roseneath/Murteree).

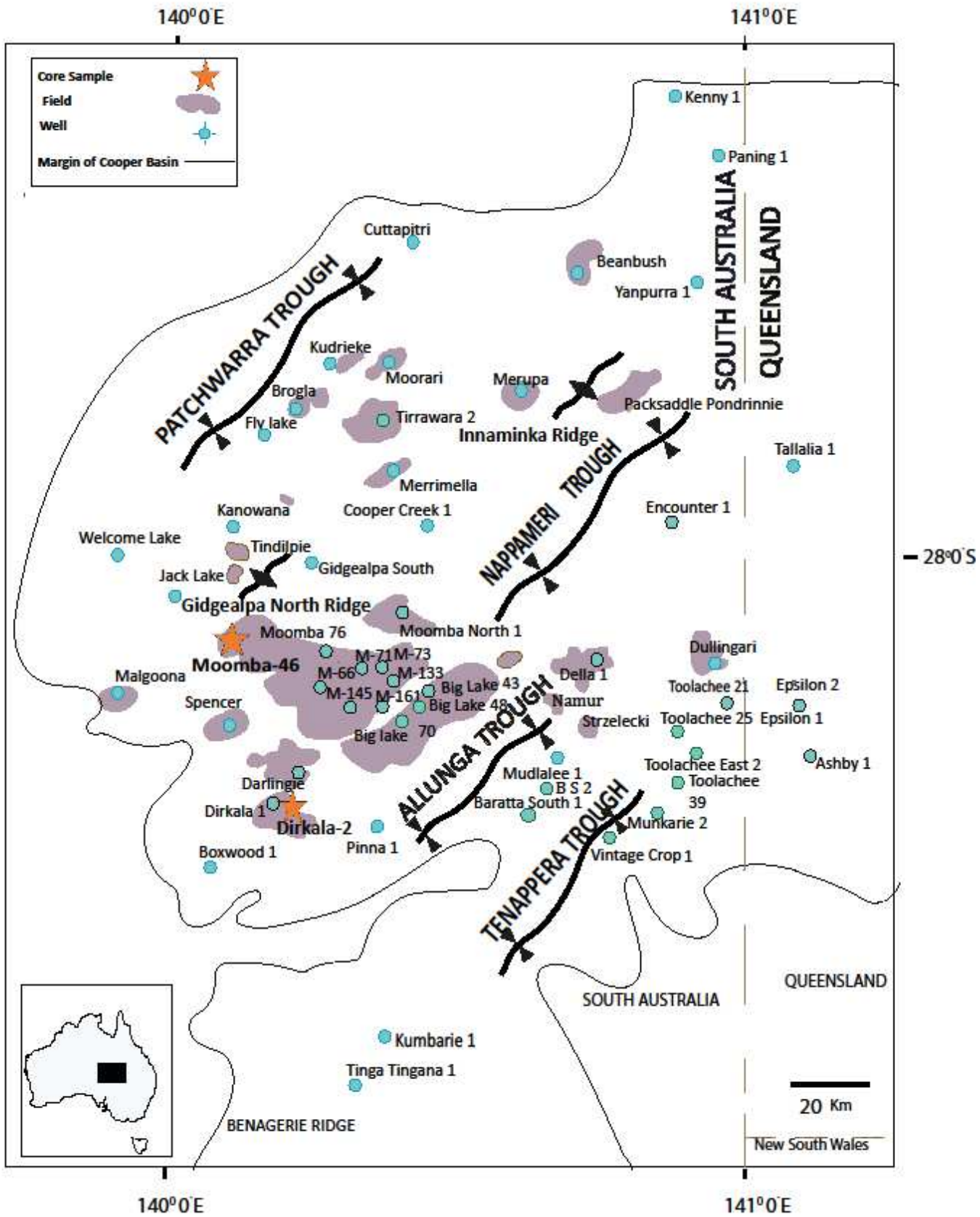

Figure 1: Map of study area showing the location of the two wells studied. In detail (star symbols) and other wells studied on the basin of electrofacies and lithologic core logs. The star symbols are core samples and blue dots well locations in the Cooper Basin, Australia (modified after Chaney et al., 1997).

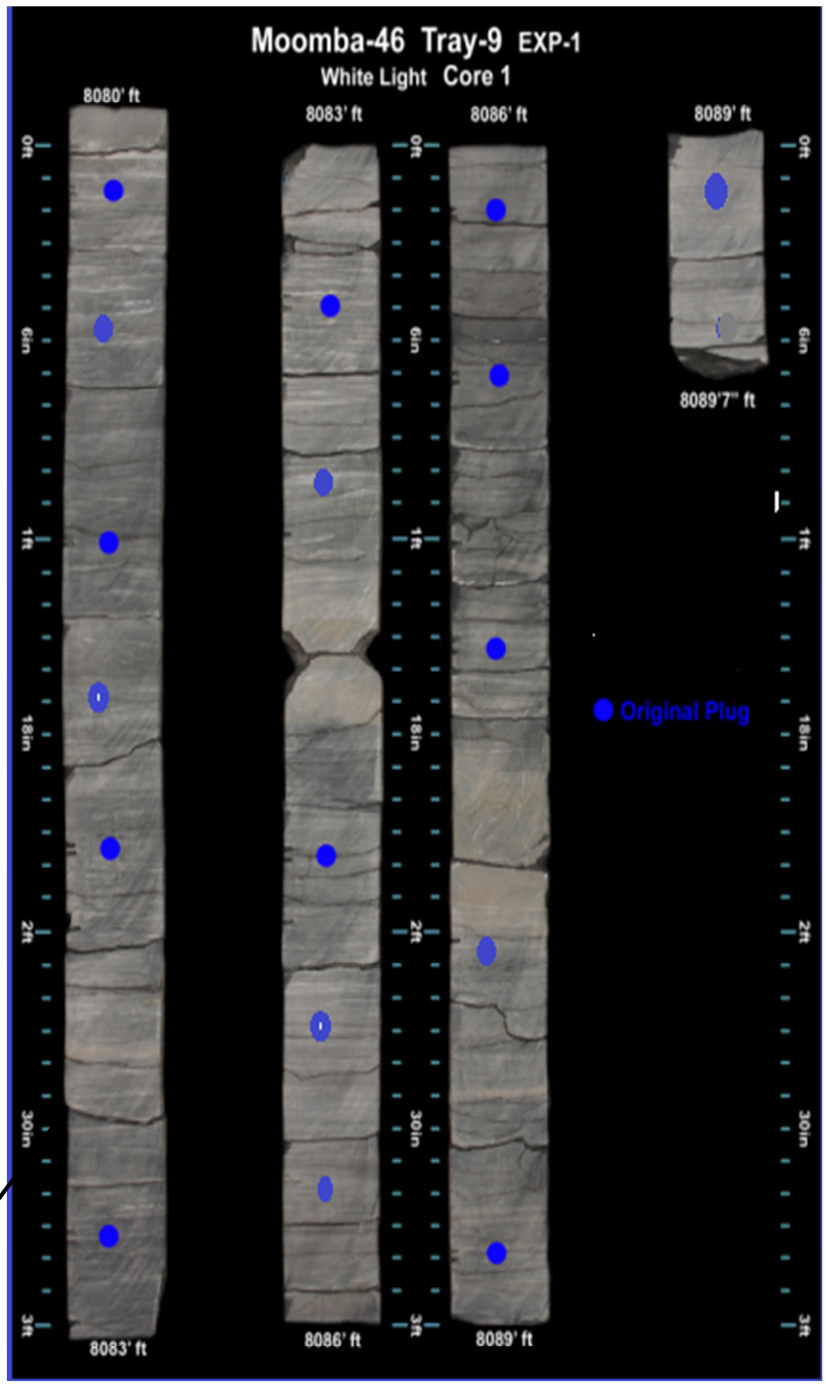

Fig-2a: Roseneath shale core, Moomba-46 well near contact with underlying Epsilon Formation

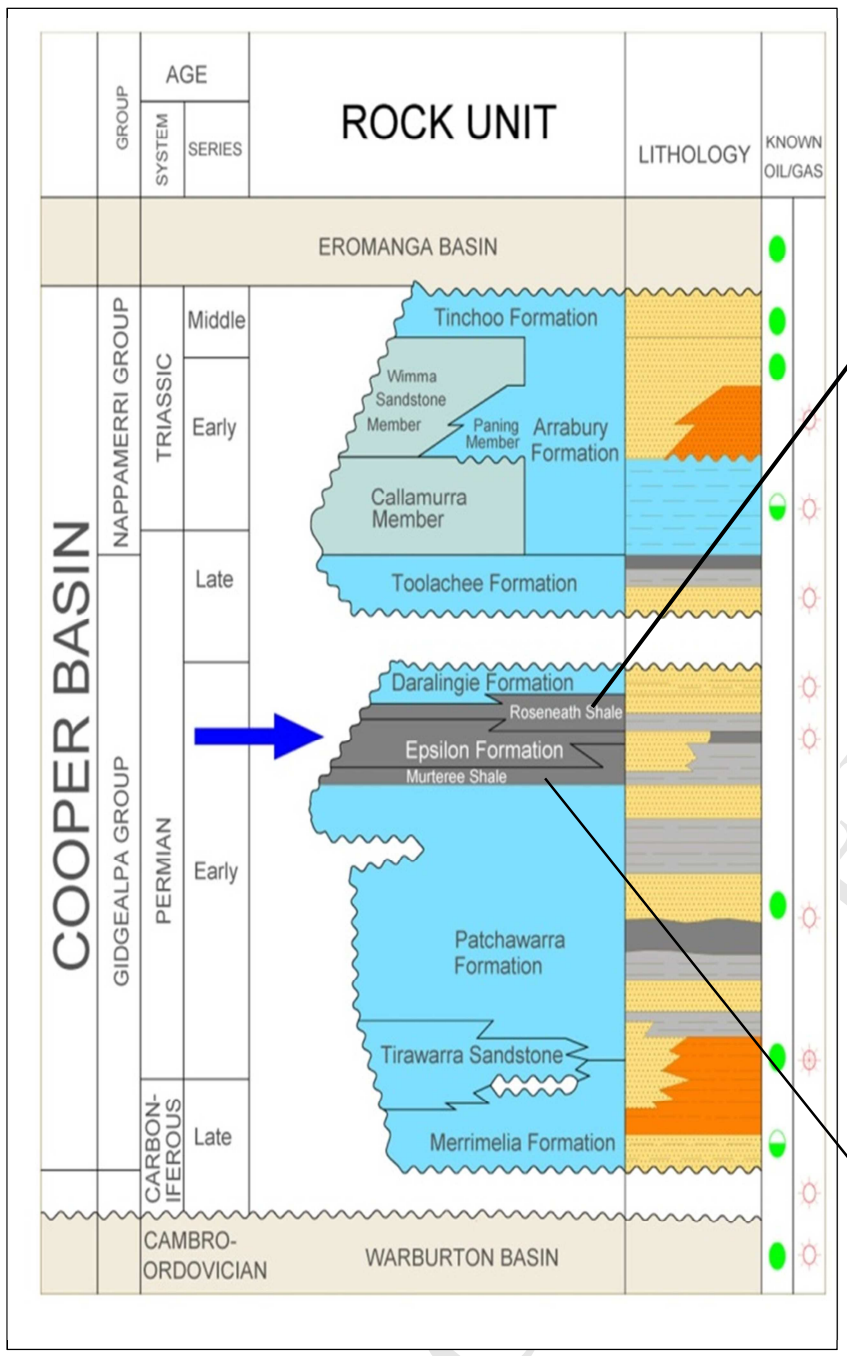

Figure 2: Stratigraphic section of the Cooper Basin (Sandra Mepes et al., 2010 South Australia (PIRSA), 2010) arrow is showing the Murteree and Roseneath Shales in bracket the Epsilon Formation and interbedded shales, siltstone and sandstones.

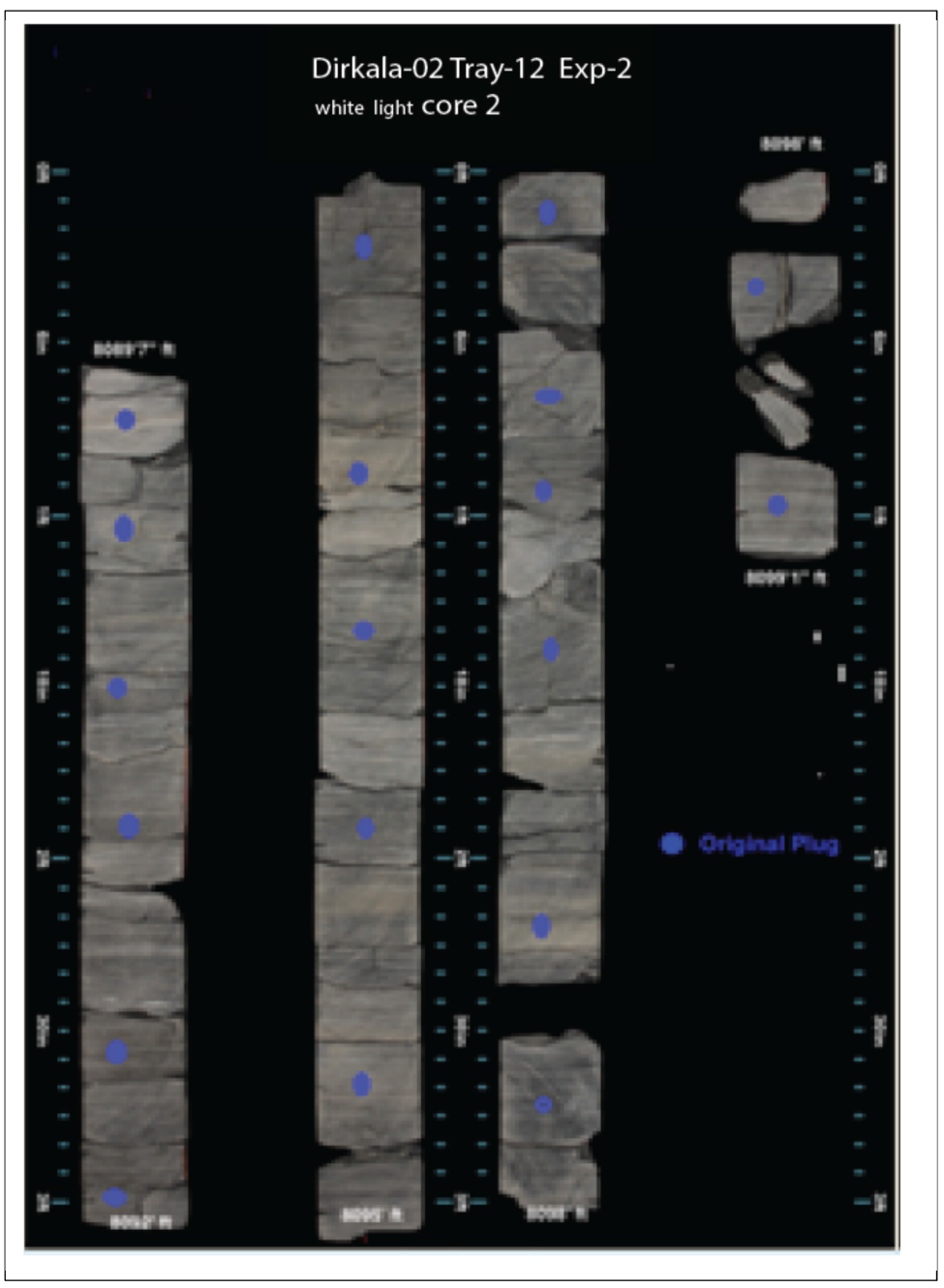

Fig-2b: Murteree shale core Dirkala -02 well near contact with overlying Epsilon Formation.

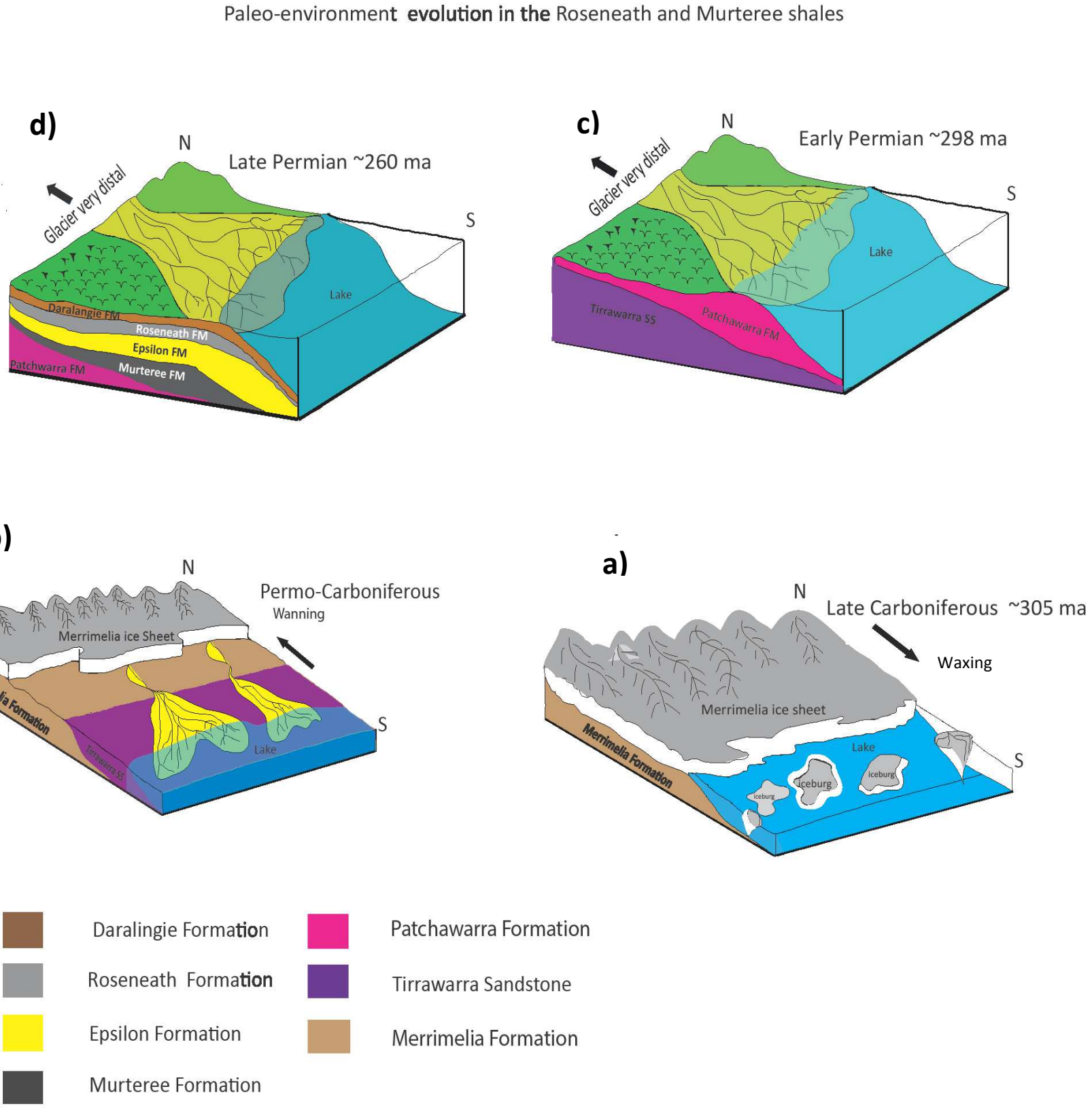

Figure 3: Block diagram illustrating four of paleo-environmental evolution Late carboniferous to Late Permian of the Roseneath and Murteree shales.

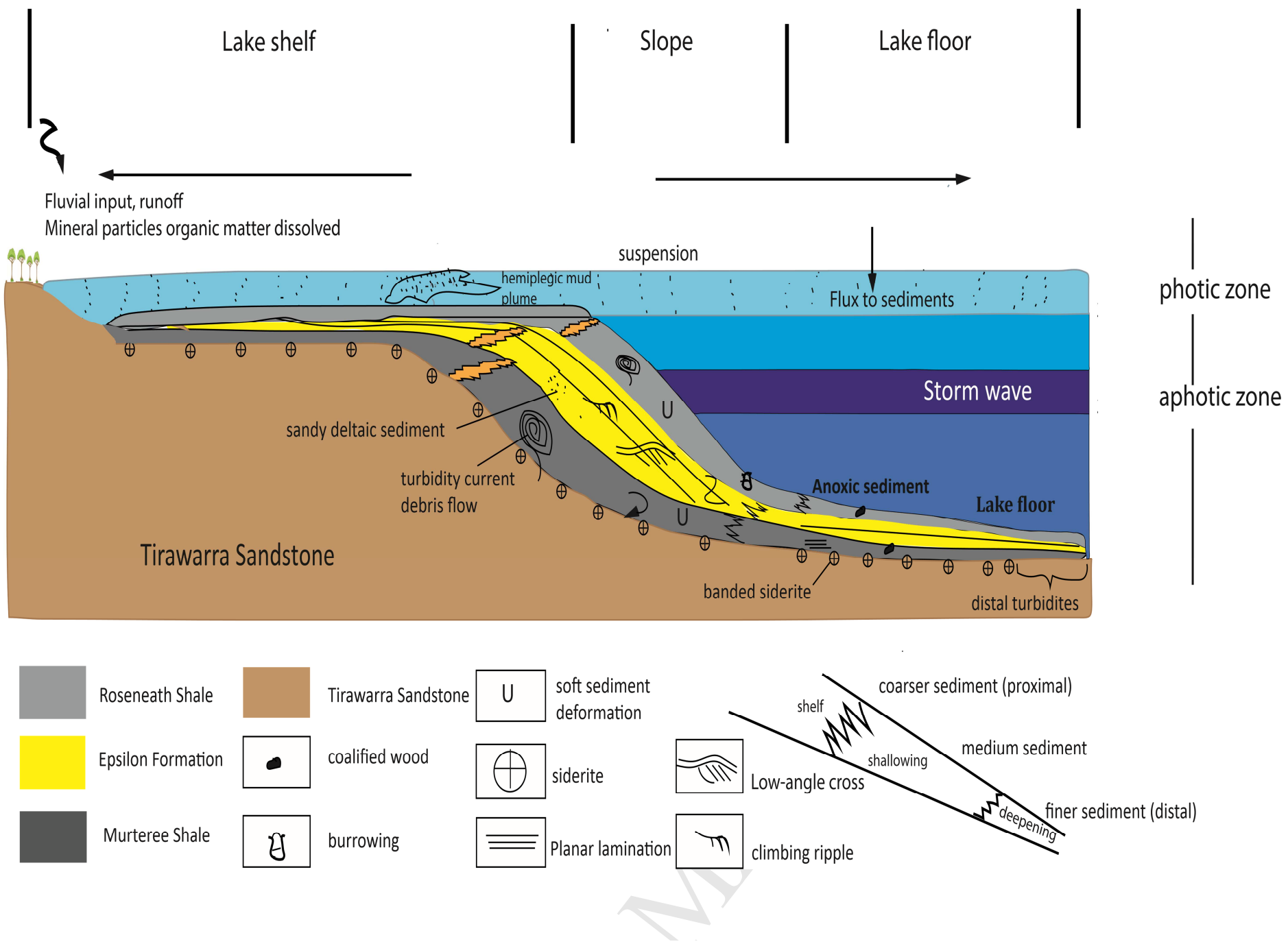

Figure 4: Conceptual model for Roseneath and Murteree shales showing depositional profile, depositional process, and plegic sediments preservation and decomposition and estimated distribution of burrowing showing. Major depositional process inferred from REM Roseneath and Murteree shales facies and sedimentary structure include suspension setting, banded siderite, turbidity currents, debris flows and gravity flow.

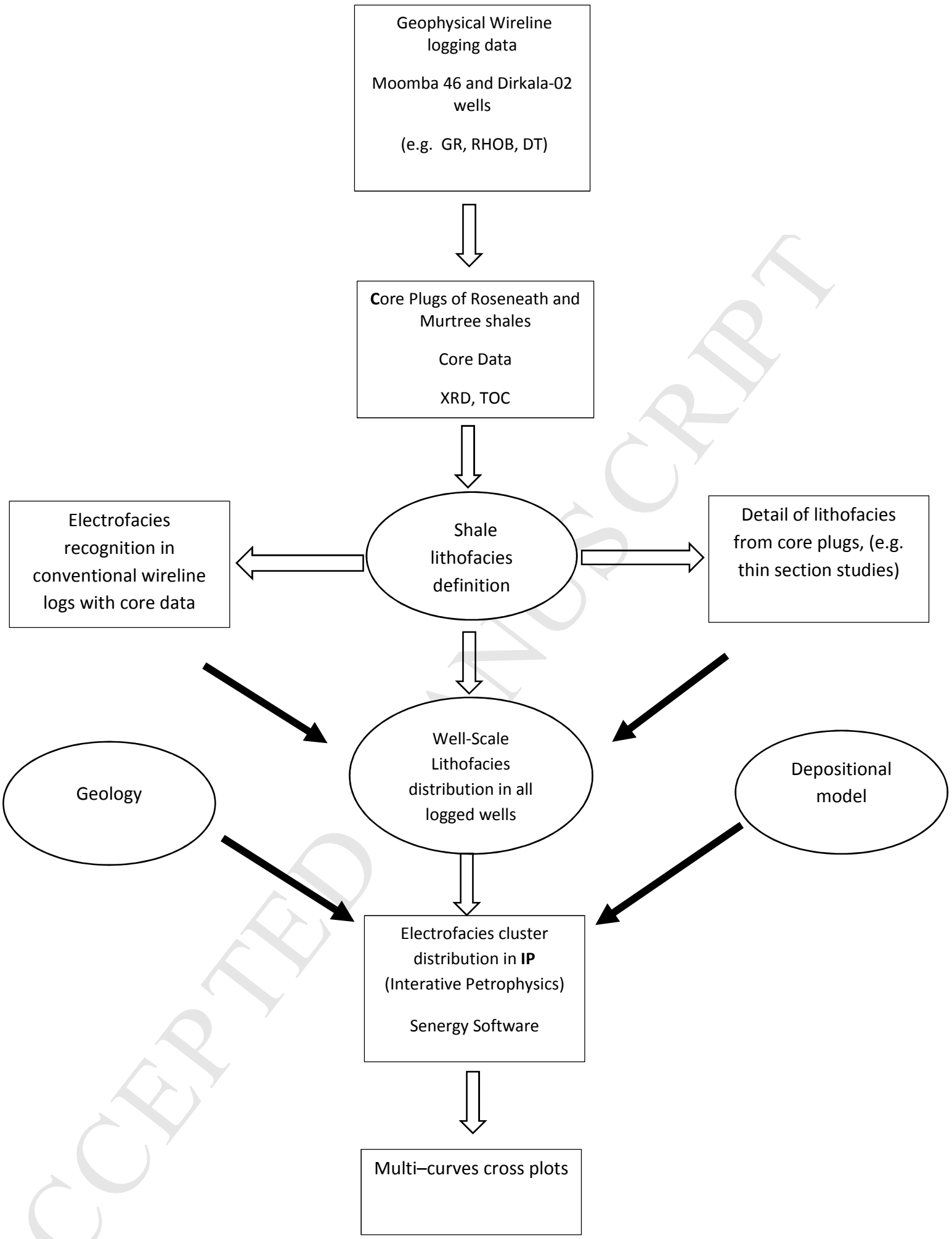

Figure 5: The workflow used in this study showing the methodology to integrate the core data, conventional wireline logs data. Lithofacies model for Roseneath and Murteree Shales in Cooper Basin.GR=gamma-ray log; PE= Photoelectric factor log; RHOB= density log; DT= sonic log; TOC= total organic carbon; XRD=x-ray diffraction.

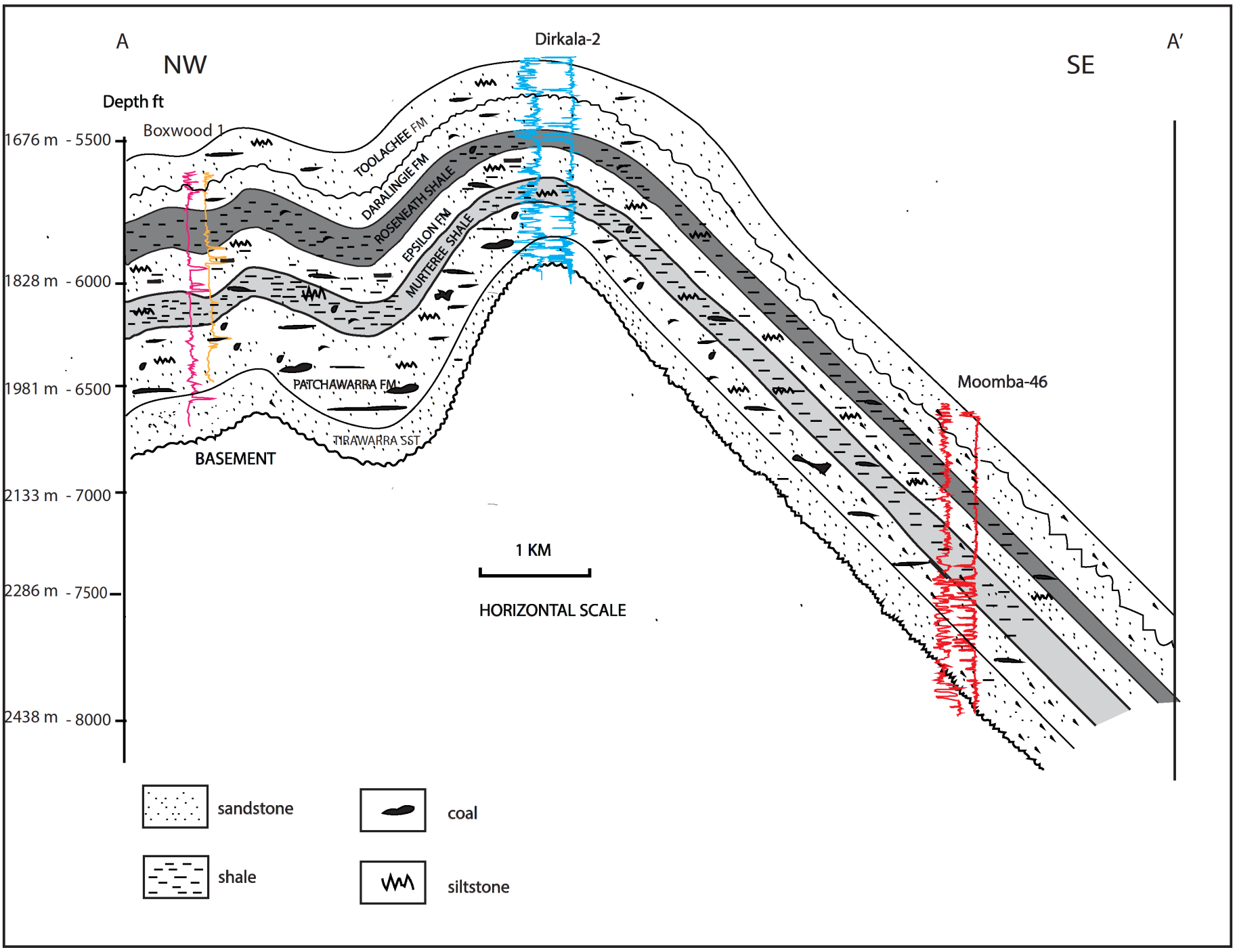

Figure 6: Structural cross-section A-A' across the Dirkal-2 and Moomba-46 wells in South Australia.

Figure 7a: Core photographs of Roseneath Shale of Moomba-46 well displaying Permian lacustrine deposits.

Figure 7b: Core photographs of Murteree Shale of Dirkala-02 well displaying Permian lacustrine deposits.

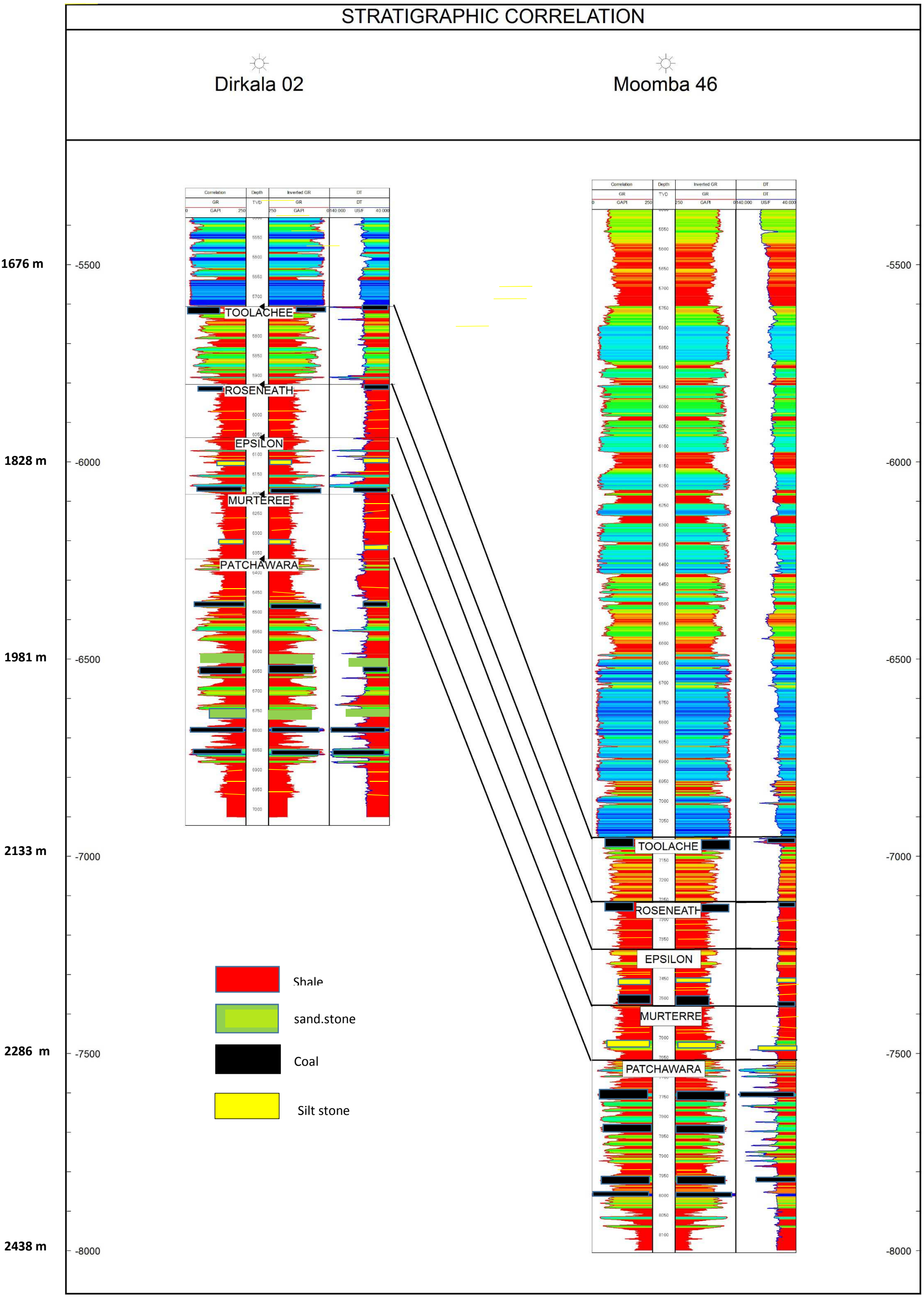

Figure 8: Stratigraphic correlation across the Cooper Basin. Gamma ray and sonic logs from Moomba 46 and Dirkala-02 showing typical correlation.

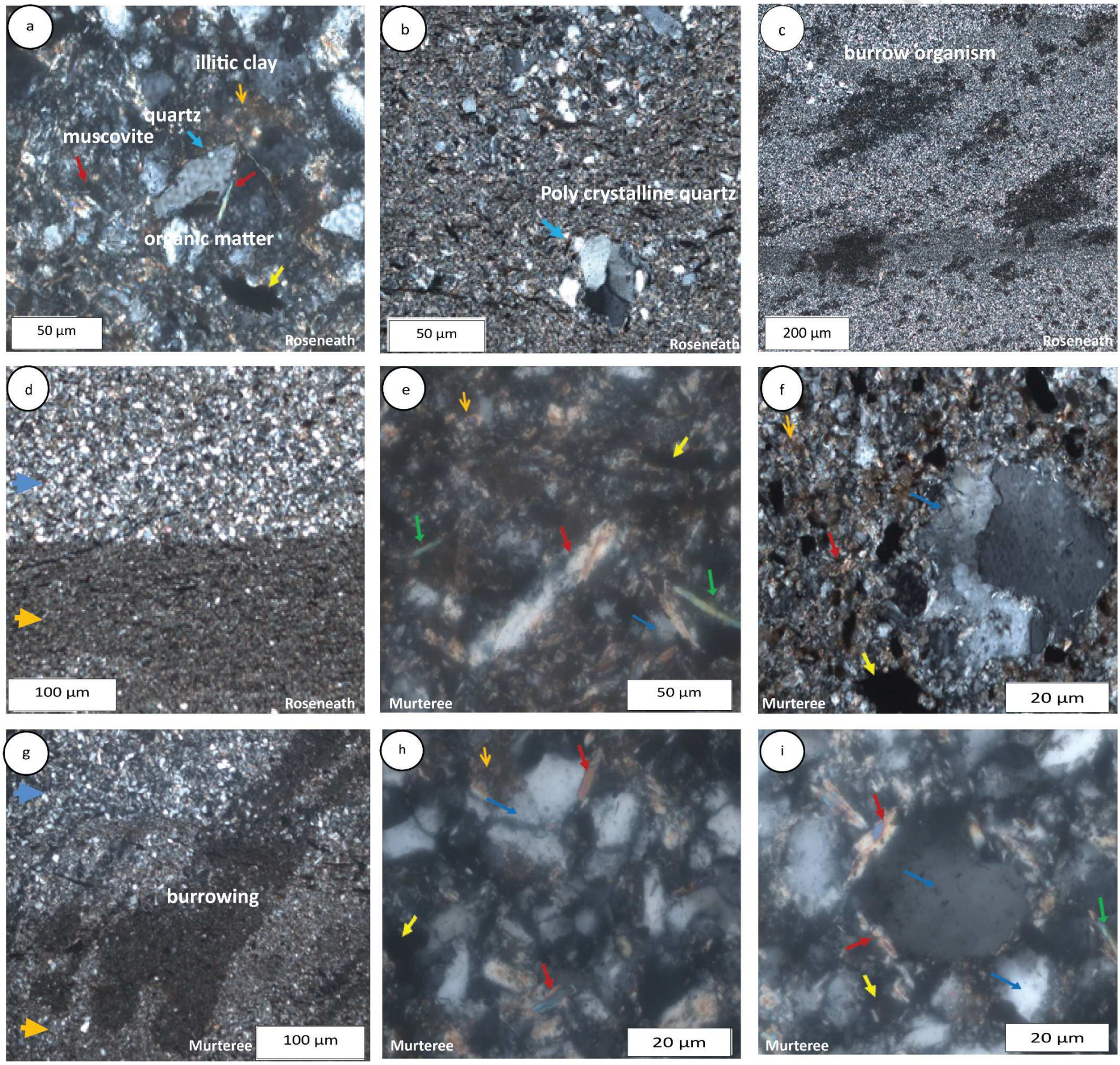
a
illitic clay
quartz
muscovite
organic matter
50 µm
Roseneath
b
Poly crystalline quartz
50 µm
Roseneath
c
burrow organism
200 µm
Roseneath
d
100 µm
Roseneath
e
50 µm
Murteree
f
20 µm
Murteree
g
burrowing
Murteree
100 µm
h
20 µm
Murteree
i
20 µm
Murteree
Quartz
Organic matter
Illitic clay
montmorrilonite
Muscovite
siderite

.

Figure 9a-i: Photomicrographs of siliceous mudstone lithofacies of thin sections (Plate-1)

a) Angular to sub-angular bunch of detrital quartz grains, muscovite and organic matter of Roseneath Shale of well Moomba-46.**b)** Clastic dominated and faintly bedded and having poly crystalline quartz (blue arrow).**c)** The photomicrograph of thin section showing tracks and trails of burrowing organisms. **d)** Organic matter along the bedding plane, it is junction between rich of silica and organic rich mudstone.
e) Thin section image at different magnification of siliceous mudstone lithofacies of Murteree Shale section of Dirkala-02 is highly rich in pore filling organic matter (yellow arrow), the white spaces seen are mostly quartz. The light green colour shows the montmorillonite, and red arrow showing the muscovite crystals.**f)** The polycrystalline quartz (blue arrow). A lot of clay material with organic lineation is observed along with quartz and muscovite in Murteree Shale well Dirkala-02.**g)**The Photomicrograph of thin section of unweathered rock showing the burrowing organism.**h)** The large grains in the middle are quartz, the white round minerals and black colour is organic matter along with brownish muscovite.**i)** The image quartz dominated unit. Again the large size of quartz grains (up to 2 mm) are surrounded by the bluish, orange muscovite (red arrow).

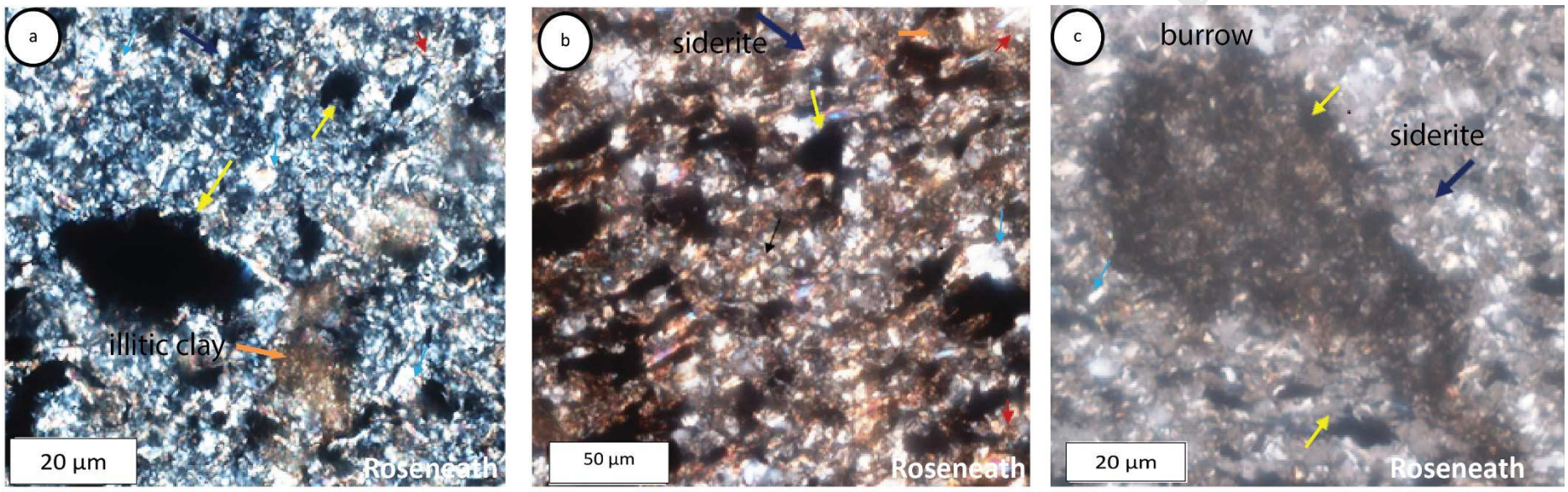

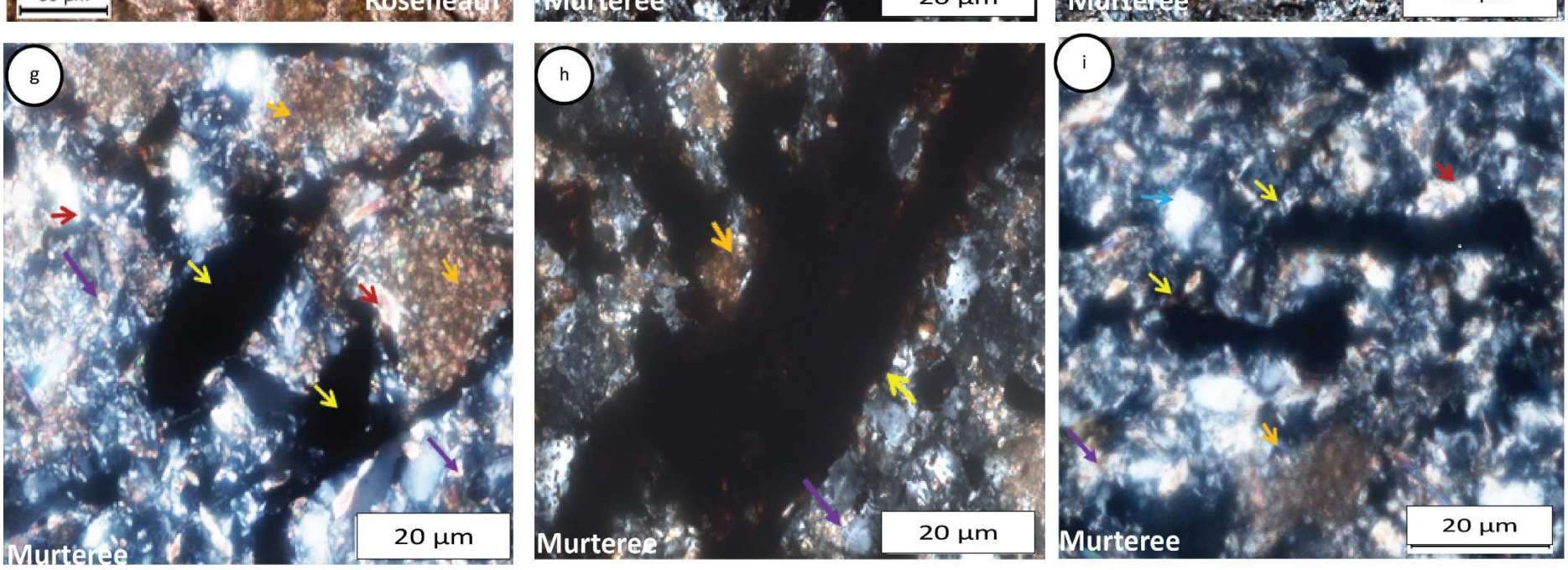

Figure 10a-i: Photomicrographs of organic siliceous mudstone lithofacies thin sections (Plate-2)

a) The Photomicrograph at different magnification image shows the high organic rich siliceous mudstone having different types of organic matter along with muscovite, carbonate-siderite and clay material are observed from Roseneath Shale, well Moomb-46.**b)** Roseneath Shale, well Moomb-46 showing the organic rich stained by darker colour organic matter (yellow arrow) consist of clay material along with siderite and muscovite. **c)** Bioturbation and digenetic activity is observed, patchy organic matter, siderite is mainly present as cement as carbonate microcretion layers together with high abundance of muscovite. Burrow penetrate down in size ~ 2mm, while the organic matter (yellow arrow) is completely burrow mottled Roseneath Shale, well Moomb-46.**d)** The Photomicrograph of Roseneath, well Moomb-46 showing disseminated black colour organic matter in homogeneous clay matrix.**e)**The Photomicrograph at different magnification of Murteree Shale, well Dirkala-2, it shows the organic rich shale. Organic matter is present as lineation. Quartz, muscovite siderite and clay patches are observed. **f)** Burrow penetrate down in size ~ 2mm, while the mudstone is completely burrow mottled. Couplets of organic matter and slightly thicker clay minerals and muscovite and bunch of quartz are observed. **g)** Illitic clay (orange arrow) organic matter (yellow arrow) gets fill the clay matrix. The red arrow shows the muscovite/biotite and black arrow shows carbonate siderite. **h)**Organic rich shale showing a well-developed massive organic material nearly 2mm wide and may be an exceptionally large. **i)** Clay minerals and particulate organic matter tube-shaped accumulate in the same sites, quartz, siderite and muscovite crystals are observed.

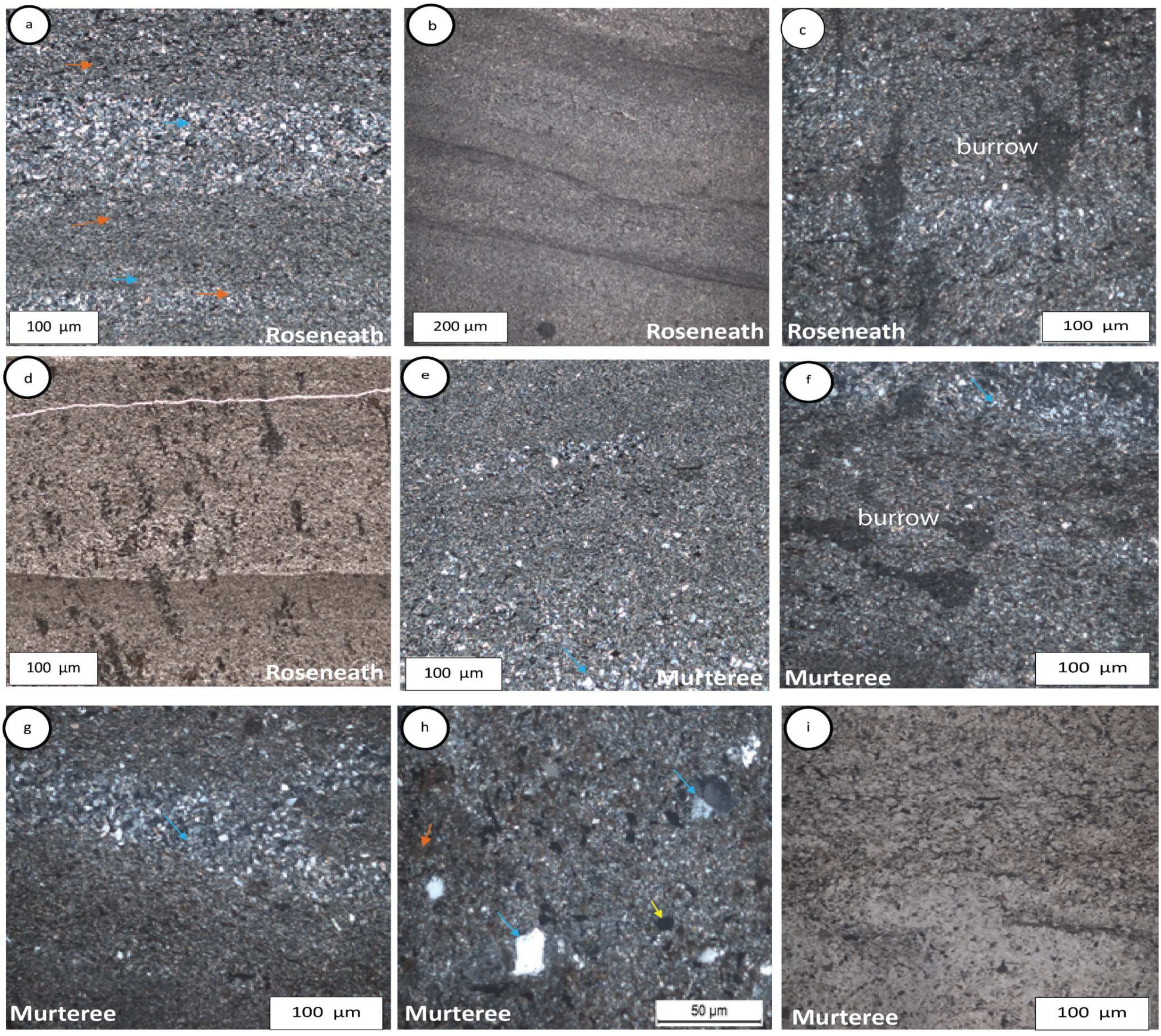

Figure 11a-i: Photomicrographs of silty siliceous mudstone lithofacies of Roseneath Shale thin sections (Plat-3).

a) Roseneath Shale, well Moomba-46 showing the symmetrical grading, generally poorly sorted, waxing then waning of flow, quartz laminae (blue arrow), alternating in siltstone layer (orange arrow).**b)** Photomicrograph of light grey to dark grey; red laminated silt mudstone, silt enrich band and clay enriched band. The base and top of the thin section are erosive-based light to dark graded, the product of low density turbidity current or upper thinner laminae from suspension or other hemiplegic. **c)** Photomicrography of silt shale poorly bedded having high bioturbation is well defined in sand-silt filled layers.**d**) Photomicrograph of laminated sandy-silty mudstone showing wavy-lenticular silt

laminae attaining with clay layer. Bioturbation in silt and mudstone. The graded silt laminae with sharp base full of burrows showing the bioturbation, grain size 0.05 mm, silt matrix. **e)** Thick to massive, poorly sorted coarse sand size quartz, channeled amalgamated of detrital quartz (blue arrow), commonly intermixed with clays are abundant (orange arrow) in the upper section.**f)** Photomicrograph burrows show the high bioturbation, burrow tube with diffused boundaries. The upper section shows the monocrystalline quartz is by the dominant mineralogical component of silt (blue arrow) lower part.**g)** Photomicrograph shows clay(orange arrow) having silt, the interbedded or channel of detrital quartz may part of erosionally based upward coarsening bed set with lenticular or wedge shaped geometry(blue arrow) lower part of the section shows the silt-enriched and clay dominated with moderate bioturbation(orange arrow).**h)** Photomicrograph shows silt dominated mudstone is characterized with polycrystalline quartz (blue arrow) and monocrystalline quartz. The section contain abundance amount of angular silt, and exhibit the disseminated organic matter and discrete be patches of silty clay (orange arrow).**i)** Photomicrograph shows the poorly bedded silty shale, silty clay is dominated in this section showing disseminated organic matter in coarse silt matrix. Darker area may be organic matter. Light area indicates relatively poor in organic matter.

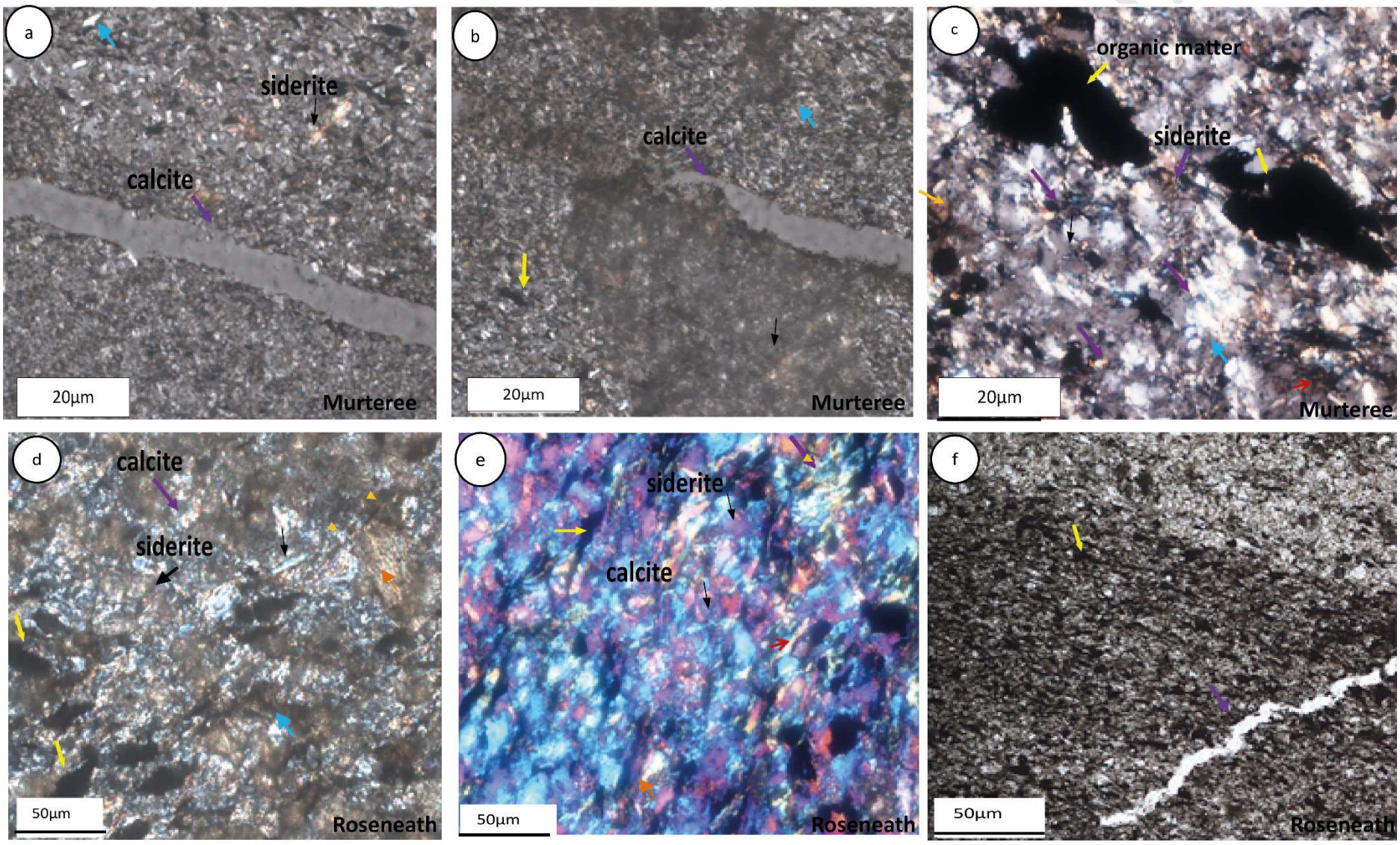

Figure 12a-f: Photomicrographs of Siliceous Calcareous mudstone lithofacies of-Murteree Shale thin sections (Plat-5).

a) The Photomicrograph shows the carbonate siliceous mudstone, Rock cut through microfracture net. It is filled with calcite (black arrow) inconspicuous microcrystalline siderite (Purple arrow) is likely admixed with clays in the silt matrix. The organic matter is disseminated (yellow arrow).The quartz grains include all the detrital material coarser than clay size particles. **b)** The microfracture is filled with calcite, underlain by the silty mudstone. Texture is dominated by the authigenic, euhedral to subhedral calcite, microcrystalline sparry calcite or sparite is significant cement in thin section. **c)** The Photomicrograph shows siderite (black arrow) appear insignificant concentration within the certain intervals in the section as replacive cement throughout the matrix along with enrich patches of organic matter (yellow arrow).**d)** The siderite (black arrow) is the most replace cement in mudstone. Authigenic or concretionary siderite most commonly forms subhedral to euhedral while calcite (black arrow). Throughout the microcrystalline matrix along with muscovite (red arrow) and organic matter (yellow arrow) are observed. **e)** The Photomicrograph siderite (black arrow) concretions appears are denser than the other lithofacies. Siderite occurs in significant as cement throughout the matrix and as a replacive authigenic carbonate mineral. Organic matter is also observed. **f)** The photomicrograph carbonate silicious mudstone in the rock matrix silt is dominated. Quartz detritic grains are visible. In the central part a microfracture can be seen filled with calspar cutting through the lamination.

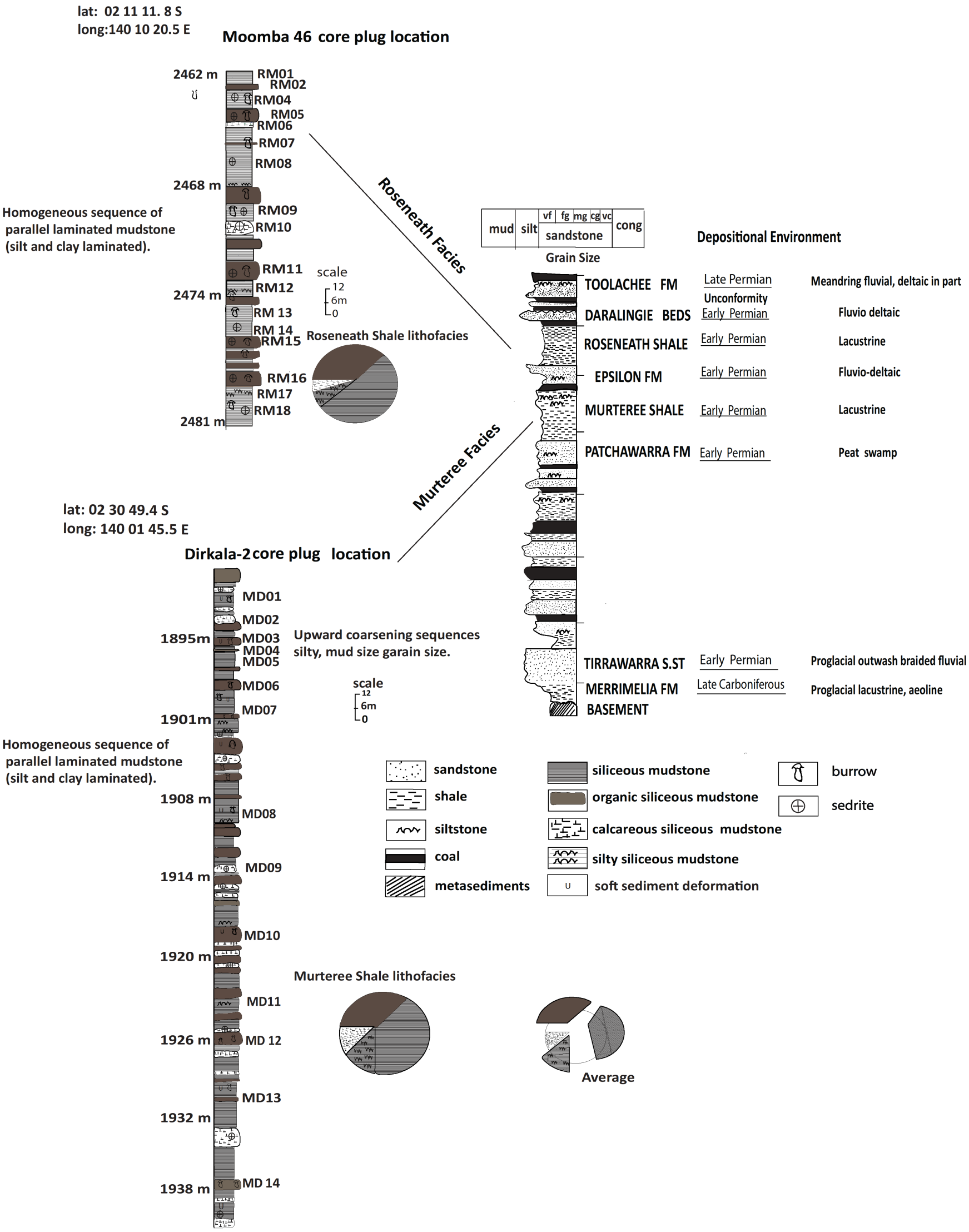

Figure 13: Lithofacies of Permian Roseneath and Murteree shales South Australia Cooper Basin core. Core description is interpreted from detailed core, wir logging data gamma ray (GR) and thin-section photomicrograph. Homogeneous sequence of parallel laminated mudstone (silty and clay laminated)

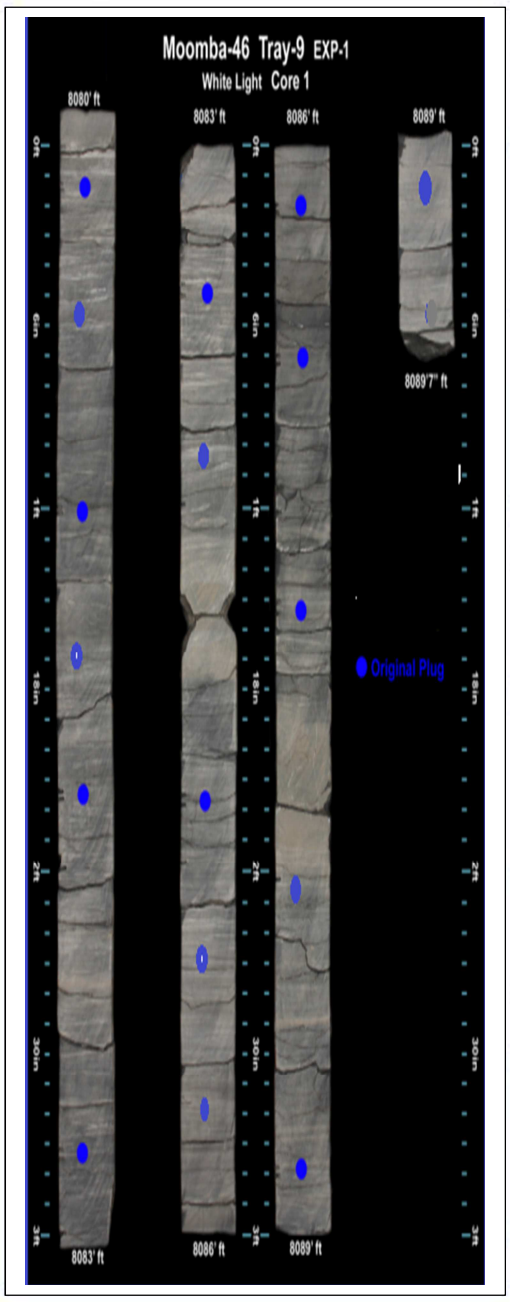

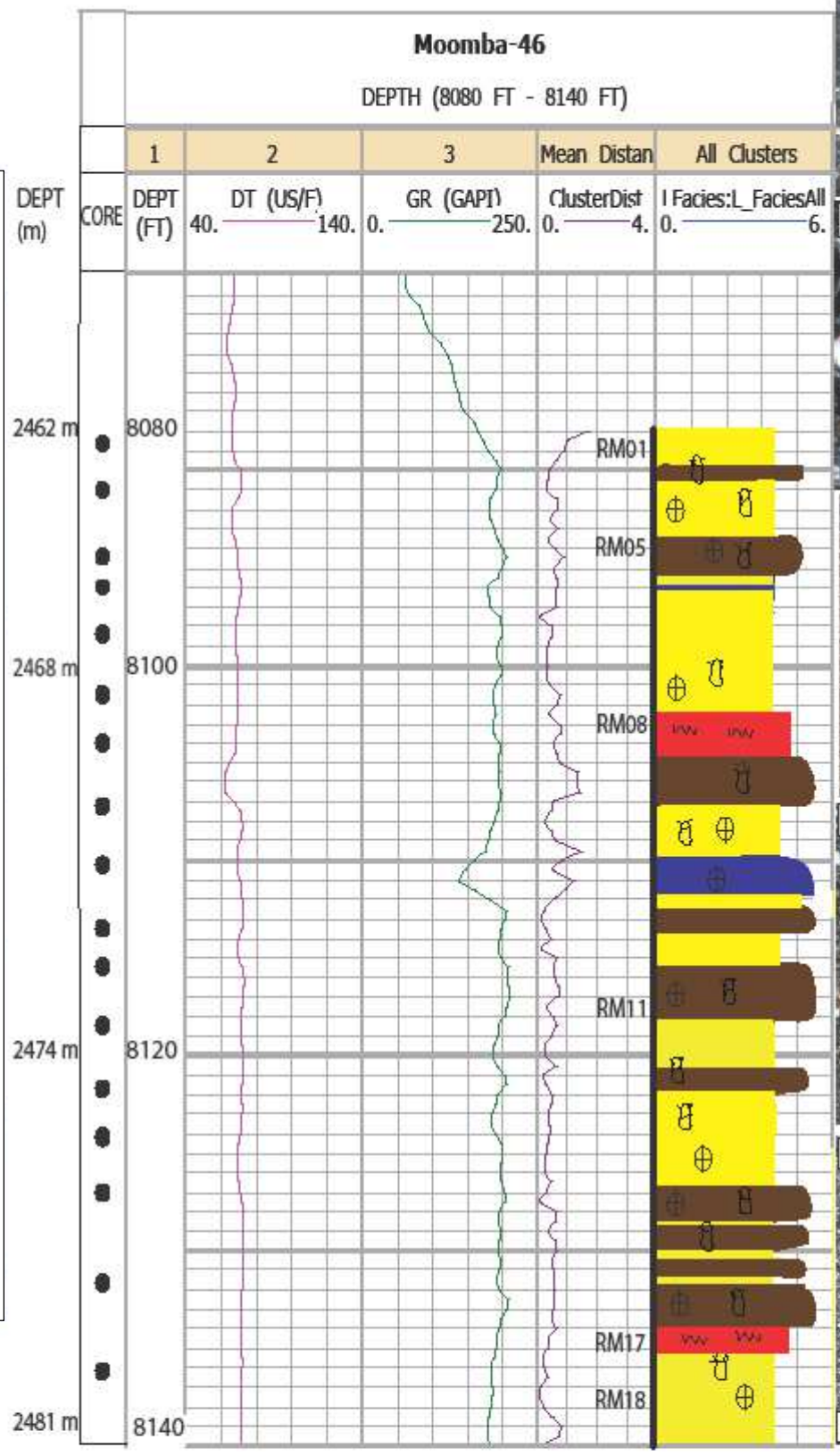

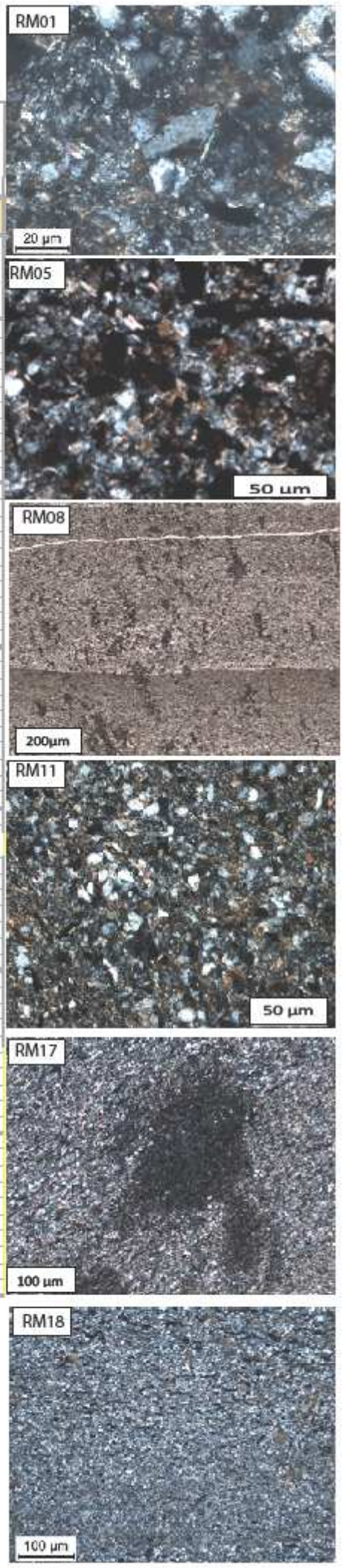

Figure 14: Example of Permian Roseneath Shale well section of Moomba 46 from Cooper Basin, showing the predicted lithofacies curves using core data and gamma ray (GR) log as conventional well log. Four predicted lithofacies curve behavior with differences. Lithofacies coded as dark brown; organic siliceous mudstone, yellow; siliceous mudstone, dark blue; calcareous siliceous mudstone; red, silty siliceous mudstone.

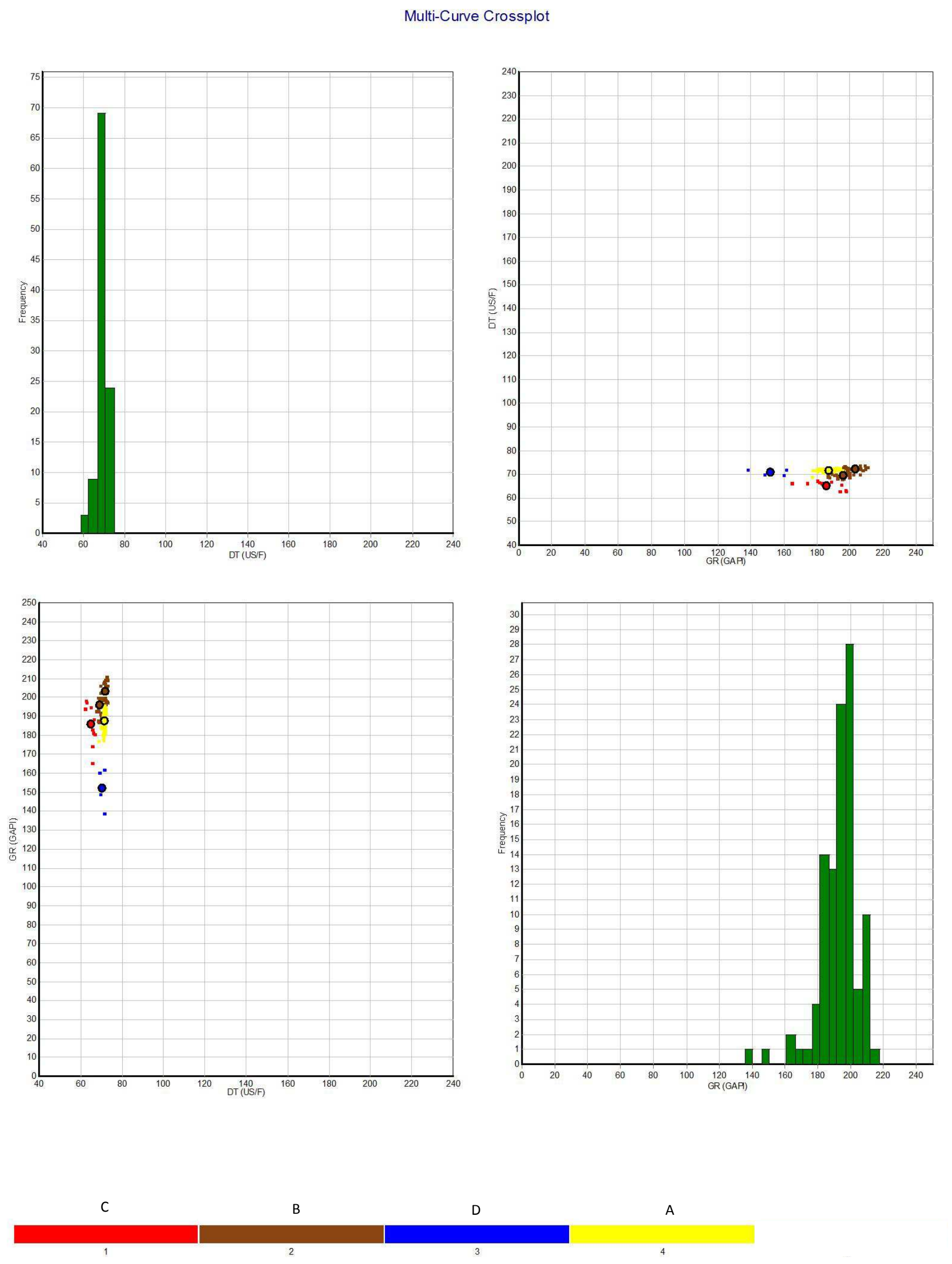

Figure 15: Distribution of the upscaled lithofacies predicted by conventional logs in Moomba 46 well Roseneath Shale. Lithofacies coded as organic siliceous mudstone, dark brown; siliceous mudstone, yellow; siliceous calcareous mudstone, dark blue; silty siliceous mudstone.

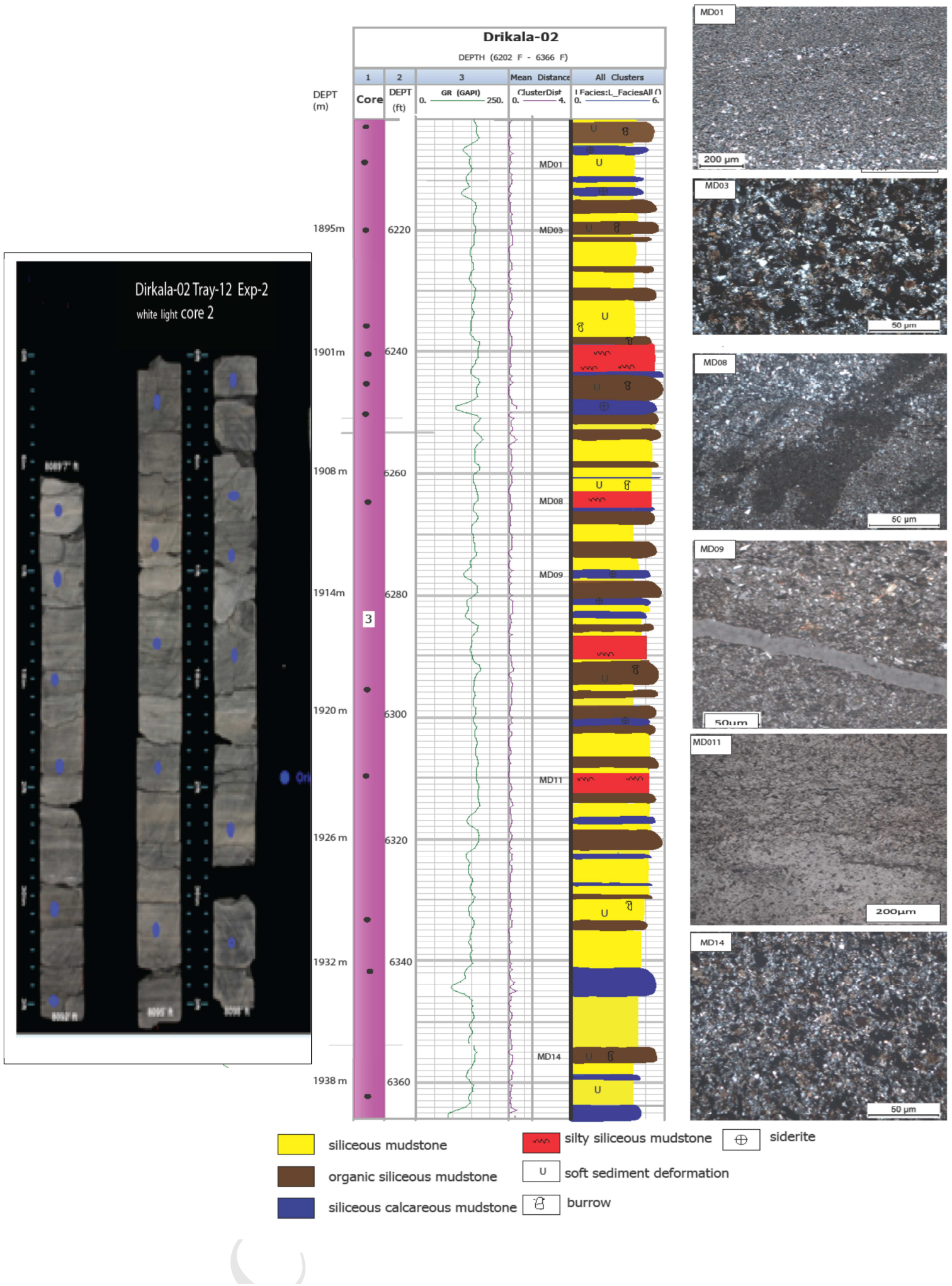

Figure 16: Example of Permian Murteree Shale well section of Dirkala-2 from Cooper Basin, showing the predicted lithofacies curves using core data and gamma ray (GR) log as conventional well log .Four predicted lithofacies curve behavior with differences. Lithofacies coded as dark brown organic siliceous mud, yellow; siliceous mudstone, dark blue; calcareous siliceous mudstone.

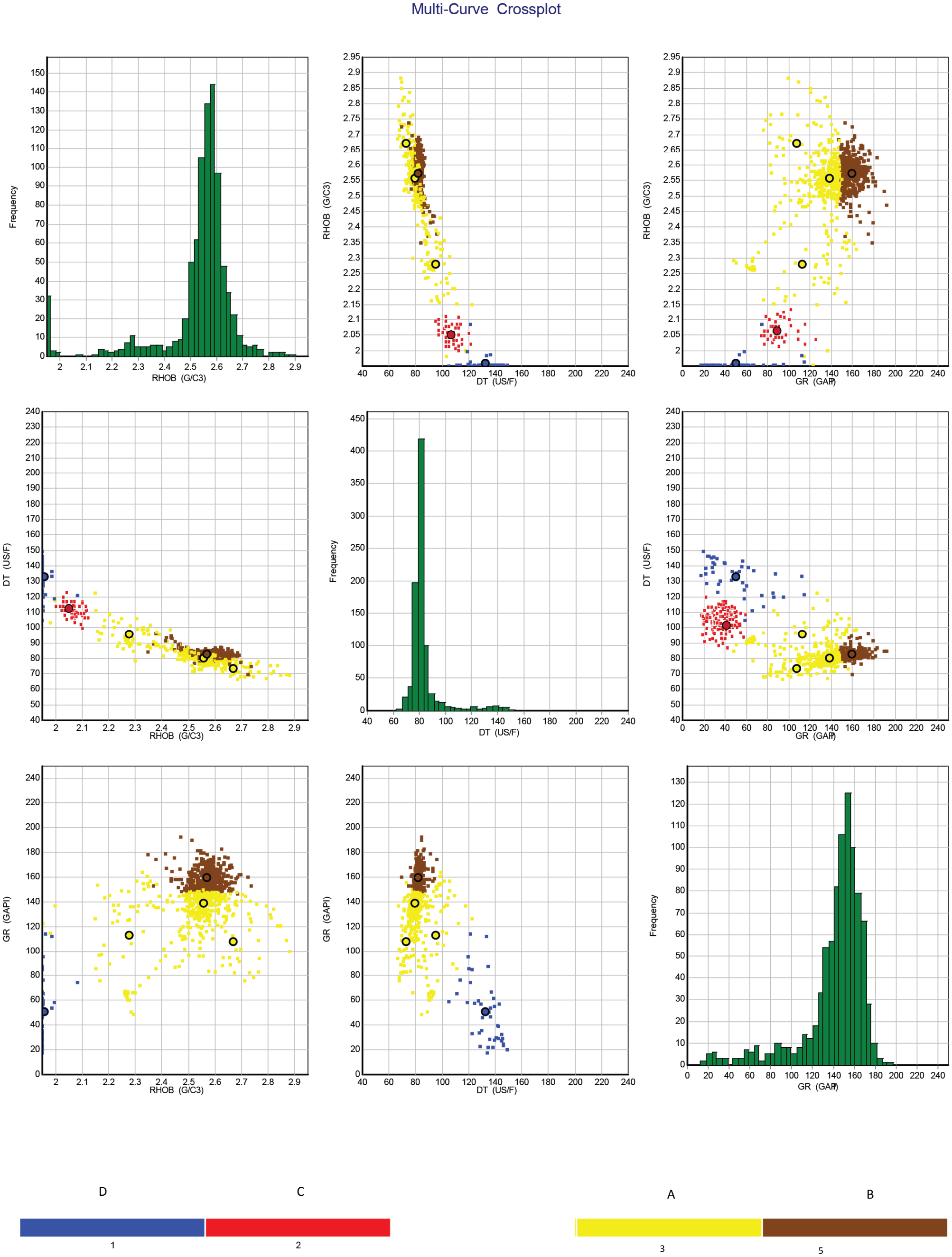

Figure 17: Resultant facies classification by clustering method. The multivariate data base of zone in Dirkala-2 well Murteree Shale at different geophysical logs. Electrofacies coded as A, yellow; B, dark brown; dark blue; C, red; D, blue.

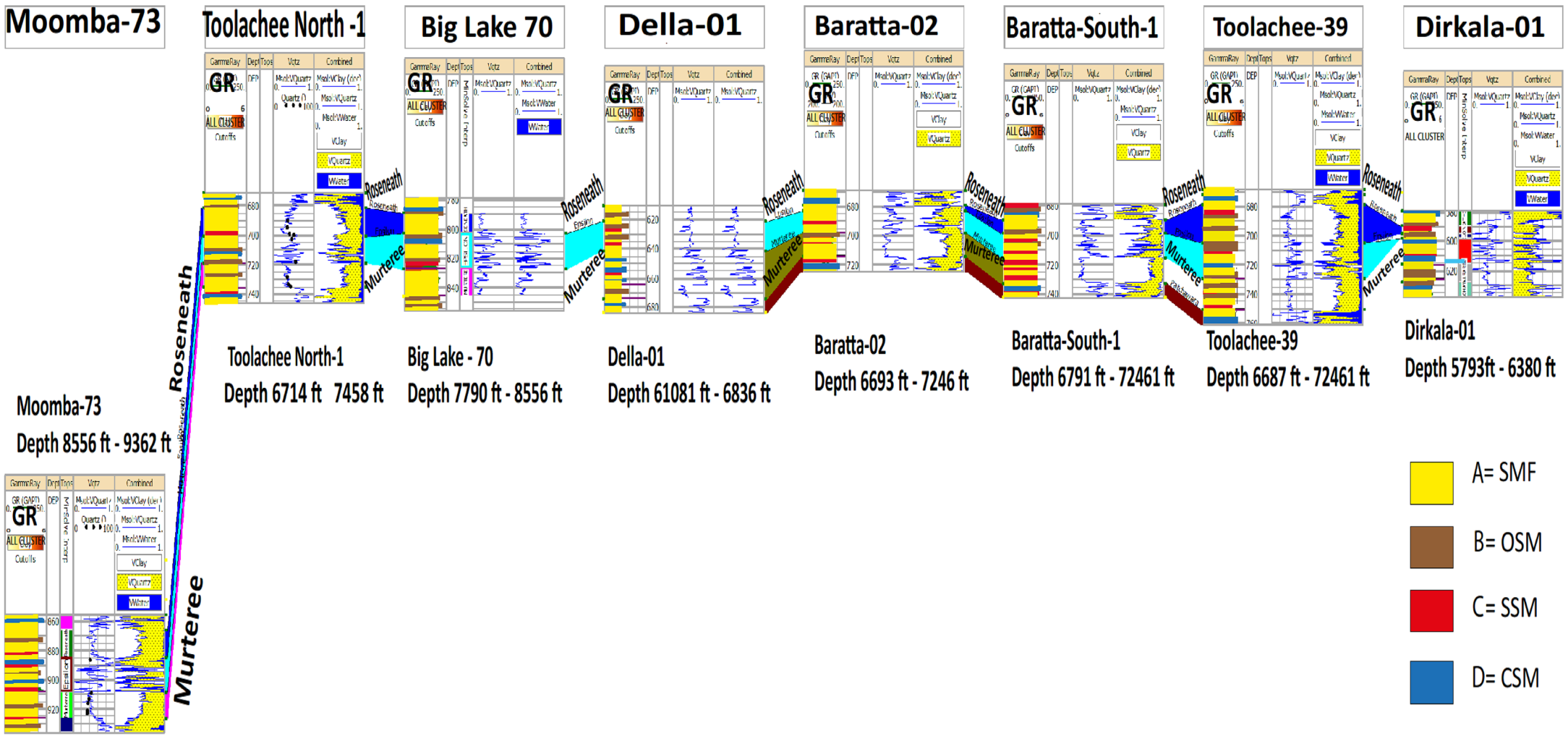

Figure 18: Distribution of the lithofacies predicted by conventional well logs of Roseneath and Murteree shales in Nappameri, Tenappera and Allunga troughs across the Cooper Basin. Electrofacies coded as A, siliceous mudstone (SMF); B, organic siliceous mudstone (OSM); C, silty siliceous mudstone (SSM); D, siliceous calcareous mudstone (CSM).

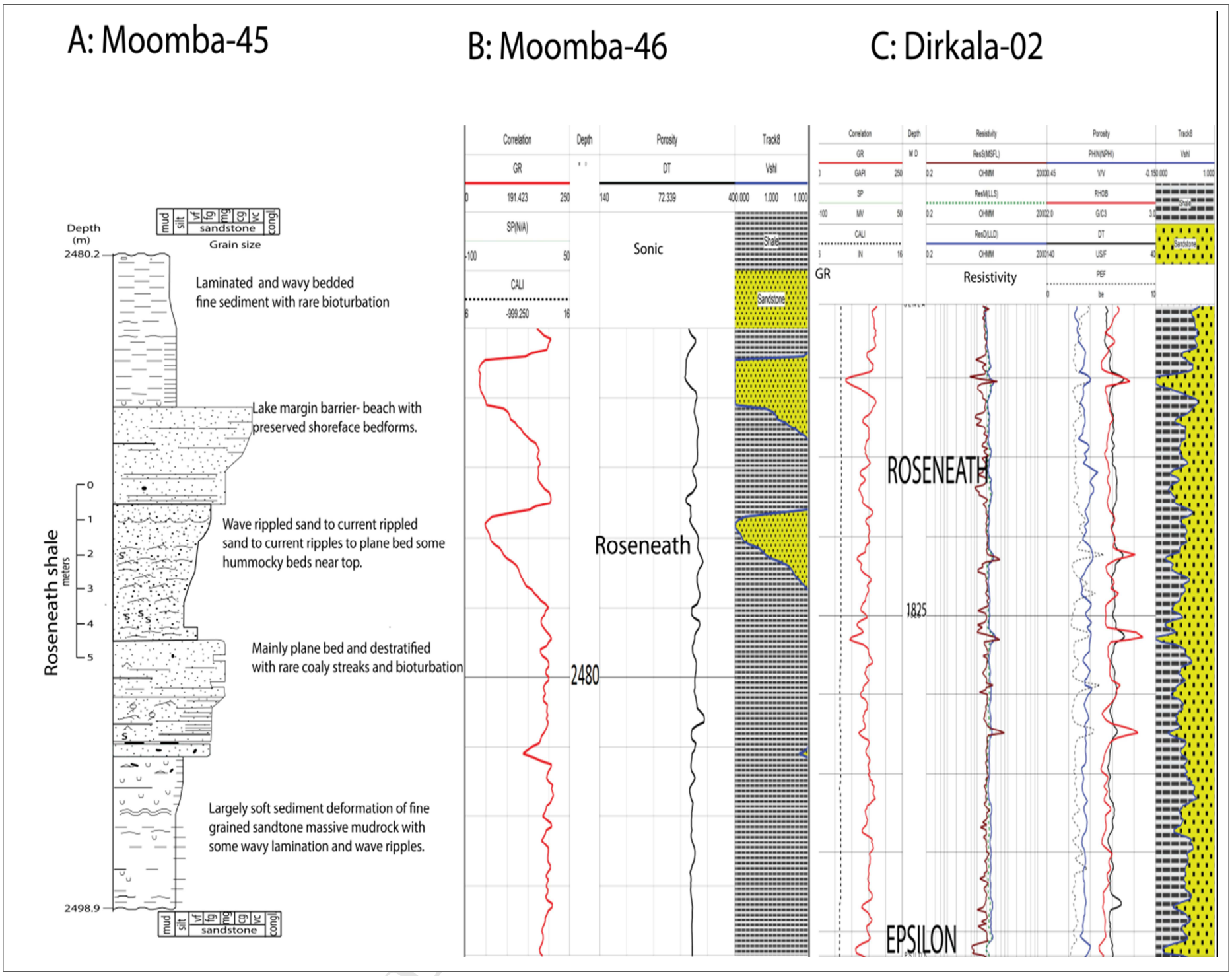

Figure 19: Sedimentary facies log of the Roseneath Shale Daralingie Formation transition, Moomba 45 modified (after Williams, 1995 & E.M.Alexander) comparison with Moomba-46, Dirkala-02.

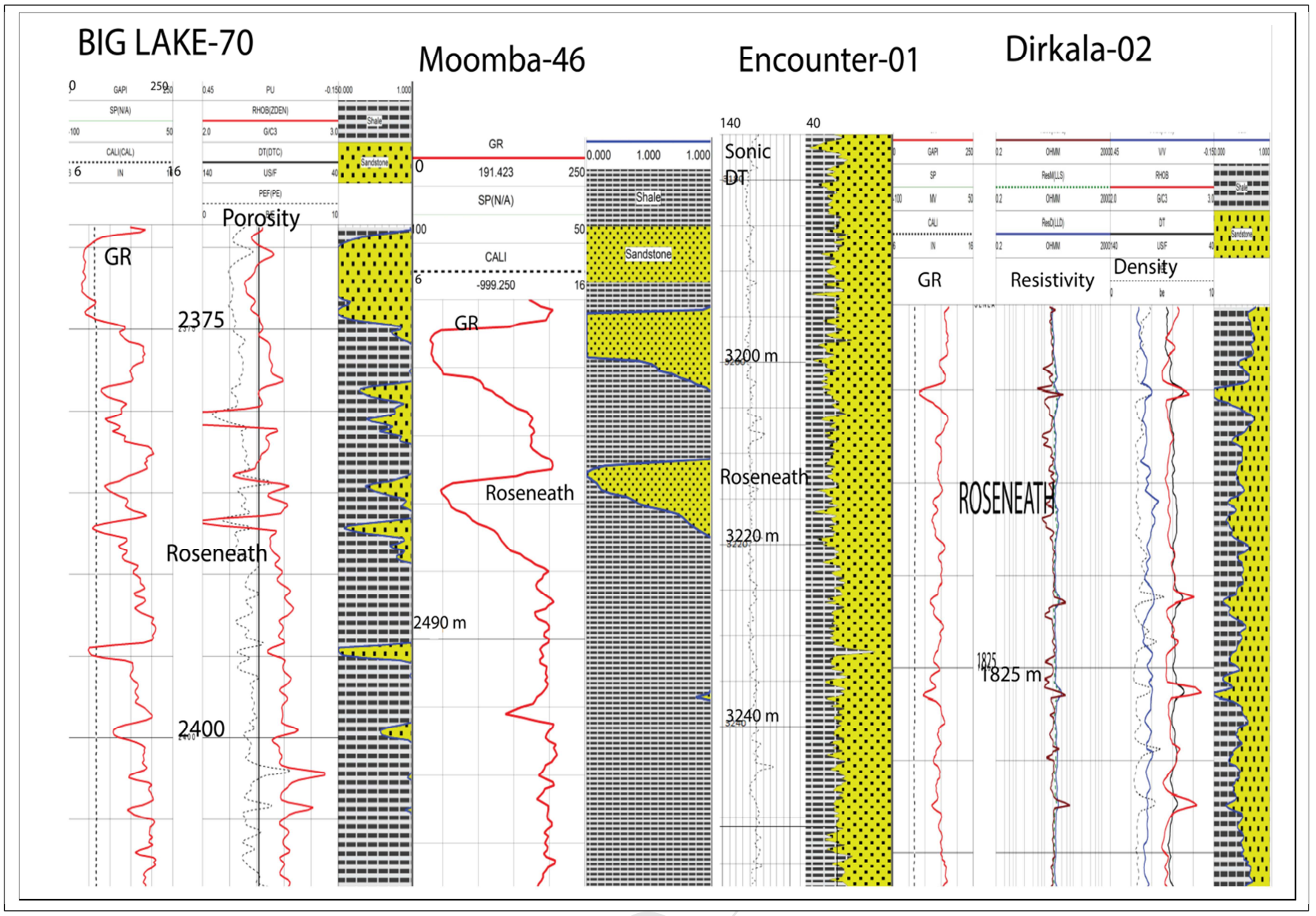

Figure 20: Sedimentary facies log of the Roseneath Shale, comparison with Big lake-70, Moomba-46, Encounter-01 Dirkala-02

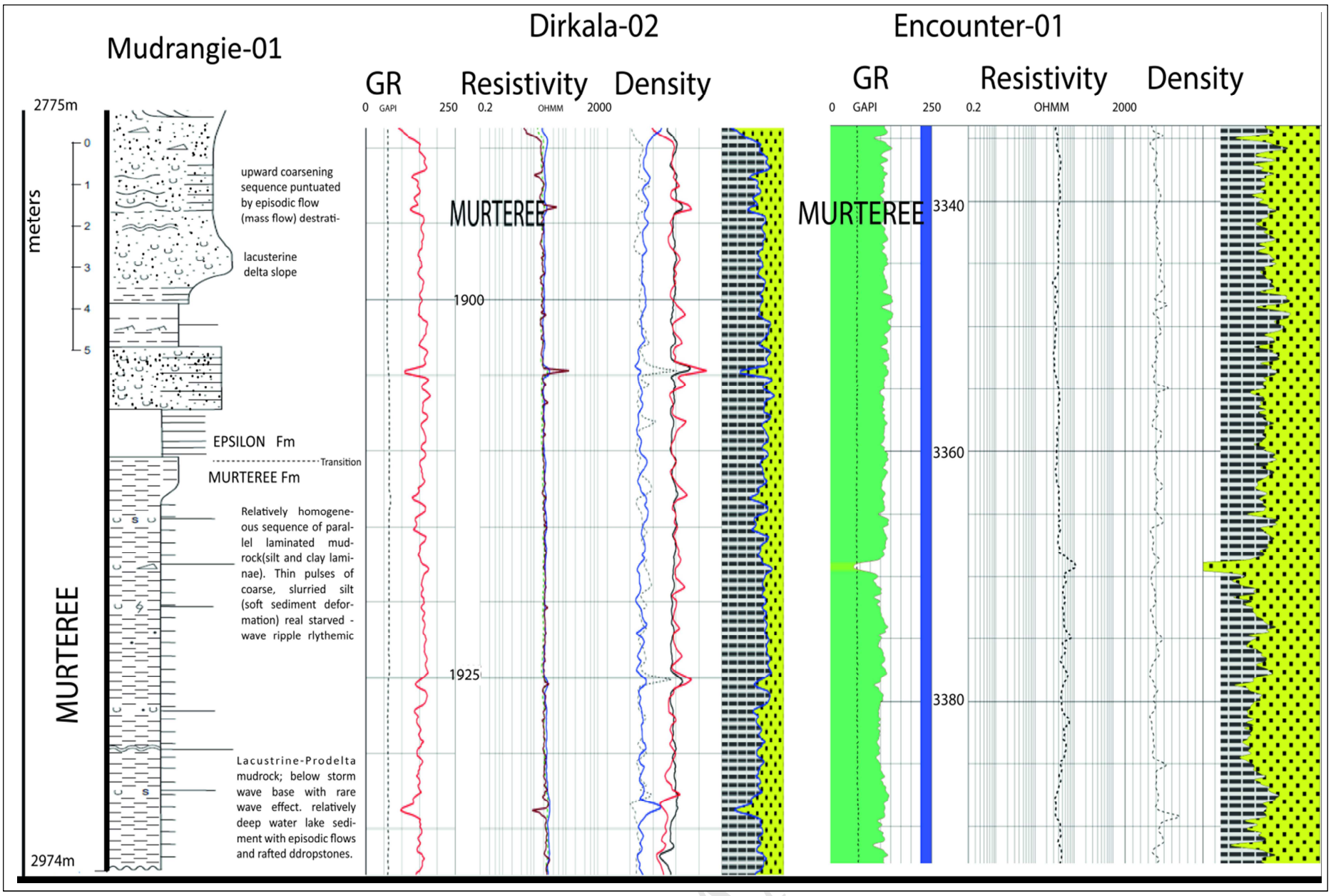

Figure 21: Sedimentary facies log of the Murteree shale- Epsilon Formation transition, Mudrangie-01 modified (after Williams, 1995& E.M.Alexander) comparison with Dirkala-02 and Encounter-01 wells).

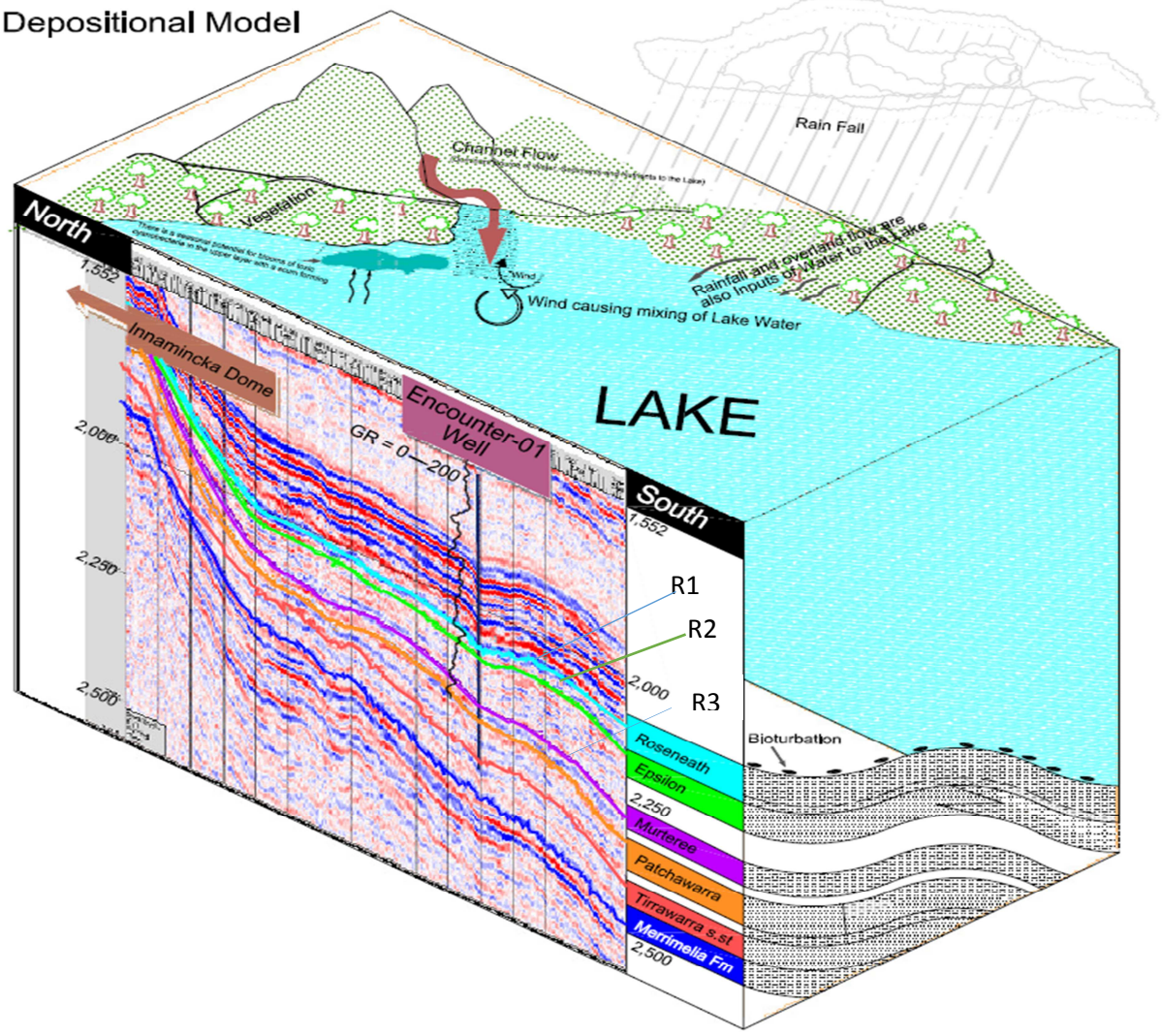

Figure 22: The depositional model of Roseneath and Murteree formations in Cooper Basin**,** Seismic traverse (North-South) from the Innamincka Dome to proposed Encounter-1, showing Encounter-1 to be down dip and outside structural closure at the Roseneath level.

- On the basis of detailed petrographic analysis of samples from two wells cored through the Permian Murteree and Roseneath shales (Dirkala-02 and Moomba-46 wells), four lithofacies have been recognized.

- The lithofacies were classified on the basis of quartz-mud ratio, grain size, sedimentary structures, and organic matter.

- Core descriptions focused on texture, lithology, bioturbation and sedimentary structure

- Petrographic and geochemical analyses of core samples are used to develop the electrofacies.

- Electrofacies modelling is used to develop a conceptual geological model of the lithofacies in areas without cored wells with the help of conventional well log data and assigned lithofacies in these wells

- Electrofacies were used to extend the facies interpretations for Roseneath and Murteree shales across the basin into areas where core was not available for study